ELSEVIER

Polymer 40 (1998) 65–93

polymer

Mechanism of the thermal degradation of prepolymeric poly(3-nitratomethyl-3-methyloxetane)

Terence J. Kemp[a,*], Zachary M. Barton[a], Anthony V. Cunliffe[b]

[a]*Department of Chemistry, University of Warwick, Coventry CV4 7AL, UK*
[b]*Defence Research Agency, Fort Halstead, Kent TN14 7BP, UK*

Revised 12 March 1998

Abstract

The thermal degradation of poly(3-nitratomethyl-3-methyloxetane), also called polynimmo, an important high-energy binder used in propellant formulations, has been examined by a variety of spectroscopic methods combined with exhaustive chromatography. Degradation results in the gradual increase in intensity of two main new absorptions around 1729 and 1550 cm^{-1} in the solution infrared (i.r.) spectrum of polynimmo. The band at 1729 cm^{-1} is attributed to the carbonyl group in a formate ester of which the associated formate proton and carbonyl carbon are clearly visible in the ^{1}H and ^{13}C n.m.r. spectra at 8.1 and 162 ppm, respectively, and can be cross-correlated by two-dimensional n.m.r. The absorption at 1550 cm^{-1} is attributed to the asymmetric stretch of a nitro group attached to a tertiary carbon. We propose that this nitro species is formed by the recombination of NO_2, following the loss of NO_2 and subsequent elimination of CH_2O from the polynimmo side-chains, with the resulting carbon radical. The assignment of this nitroalkane was confirmed by electrospray mass spectrometry, (including collision-induced decomposition studies) and n.m.r. spectroscopic characterization of a nearly pure sample of the cyclic tetrameric nitro species isolated from pyrolysed polynimmo using column chromatography. Degradation also results in the development of a strong electron spin resonance absorption attributed to a nitroxide radical produced in a secondary reaction.

Keywords: Binder; Thermal degradation; Polynimmo

1. Introduction

The performance of composite propellants, which comprise a fuel, such as a hydrocarbon or aluminium powder, an oxidant (often ammonium perchlorate) and an organic host matrix or 'binder' (usually a flexible organic polymer), can be enhanced by making the binder an energetic material in its own right, e.g. by incorporating a nitrate ester group. Poly(3-nitratomethyl-3-methyloxetane), also known as polynimmo, is such a binder [1]. This is synthesized [1,2] as a viscous liquid prepolymer which is cured to a rubbery solid on curing with a polyisocyanate, namely Desmodur-N100 [1–3]. Polynimmo has been shown [4] to be a complex mixture of oligomers, both linear,

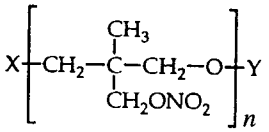

(where X and Y are various end groups), and cyclic,

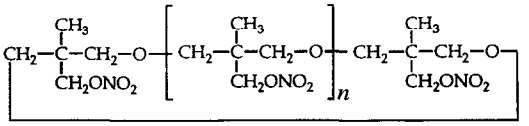

where n reaches a value of 20.

One problem resulting from the use of nitrated organic molecules as binders is their relative thermal instability [1,2,5,6], particularly in hot climates, and stabilizers such as 2-nitrodiphenylamine are added to the formulation at 1–2% levels [2].

Mechanistic studies of the thermal decomposition of polynimmo and other nitrate esters of polyethers are few. Analysis has been carried out of the gases evolved during the pyrolysis at 100°C of cured polynimmo [6], while Farber et al. [7] have made a mass spectrometric study of the pyrolysis at 150°C of 3,3-bis(methylnitraminomethyl)oxetane (BMNAMO) and, to a lesser extent, polynimmo. Other studies relate to the kinetics of weight loss and simultaneous mass and temperature change, (SMATCH)-*FT*i.r. spectroscopy [8–10]. (Here

* Corresponding author.

0032-3861/98/$ - see front matter
PII: S0032-3861(98)00276-6

the data were obtained at heating rates more than 100 K s^{-1} to simulate the combustion of the bulk material in a rocket motor: rapid-scan *FT*i.r. spectroscopy is used to identify the gaseous products near the surface of heated polymer films.)

Cognate studies are those relating to the thermal decomposition of nitrocellulose [11] and simple nitrate esters [12]. The consensus of opinion is that O–NO_2 bond scission is a dominant feature for both types of material. For the simple nitrate esters, this is often followed by loss of formaldehyde and ring closure, e.g. for nitropentaglycerin [12],

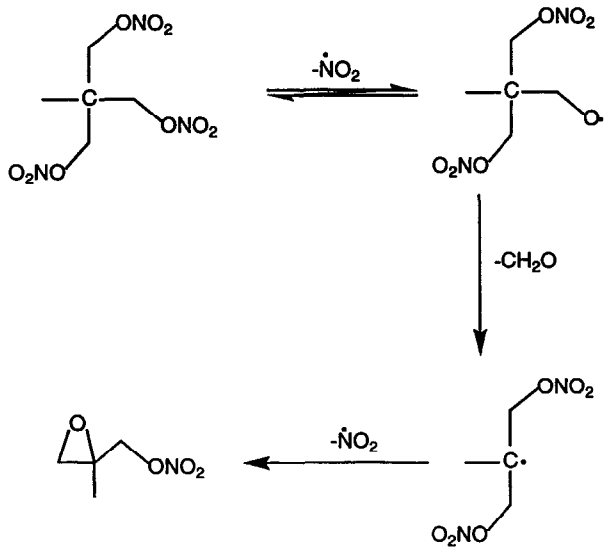

Loss of NO_2 in a primary step to produce an alkoxy radical can, however, be followed by its recapture from the solvent cage, as in the case of neopentanol nitrate [12],

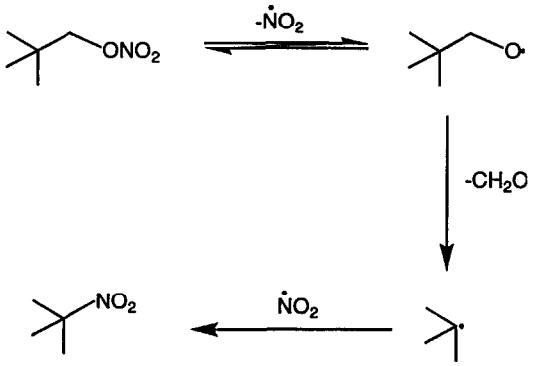

In the present study, the thermal decomposition of polynimmo has been studied by a variety of spectroscopic methods and the products detected have been explained in terms of some of the mechanisms outlined above for other types of nitrate ester.

2. Experimental

2.1. Materials

Polynimmo was received from the Defence Research Agency, having been supplied initially by ICI (Explosives Division). In general, the various batches had M_w in the range 3000–3700 and M_n in the range 1600–2000 Da. Solvents for ESI experiments and crystalline materials for MALDI experiments were of the highest grade commercially available.

2.2. Column chromatography

Pyrolysed polynimmo was chromatographed on a glass column (1 m × 5 cm) filled with a toluene (h.p.l.c. grade)-silica (particle size 0.040–0.063 mm (230–400 mesh ASTM) from Merck) slurry. Polynimmo (5.0 g) was dissolved in toluene to give a saturated solution and pipetted on top of the silica to a depth of *ca* 3 mm. A layer of sand (Fisons, 40–100 mesh, low in iron) was placed on top of the polynimmo to avoid disturbance during solvent addition. Toluene was then added continuously to the column while the eluate was collected in 15 cm^3 fractions: this extracts the less polar constituents of the pyrolysate. Methanol–toluene mixtures, with a gradually increasing methanol component (up to a maximum of 10%), were then added to elute the more polar components. Normally 100 fractions were collected using toluene as eluent and another 100 using the methanol–toluene mixtures. The solvent was removed from each fraction on a rotary evaporator and the (polymeric) residue analysed by n.m.r., SEC, i.r. and ESI.

2.3. Electrospray ionization (ESI) mass spectrometry

Spectra were recorded on a VG Quattro II spectrometer as described in our earlier publication [4] on characterization of polynimmo.

2.4. Size exclusion chromatography

The size exclusion chromatography (SEC) used in this work consisted of a dual piston high pressure liquid chromatography (h.p.l.c.) pump (ICI Instruments LC1110). The data were collected using a Polymer Laboratories (PL) data capture unit (DCU) and analysed using PL Calibre SEC software.

The SEC eluent was THF with a flow rate of 1.0 ml min^{-1}. Toluene (0.2 wt%) was used as an internal standard and flow marker in each sample. All samples were examined at equal concentrations (5 g dm^{-3}) except where otherwise stated. The column set consisted of a Pl 5 μm bead size guard column (50 × 7.5 mm) connected to a Pl 3 μm bead size Mixed-E column (300 × 7.5 mm). The system was calibrated with poly(propylene oxide) (PPO) standards.

2.5. Electron spin resonance spectroscopy

Electron spin resonance spectra were measured on a Bruker Model ER 200 tt instrument. Field calibration was carried out using *g*-tensor standards as described before [13].

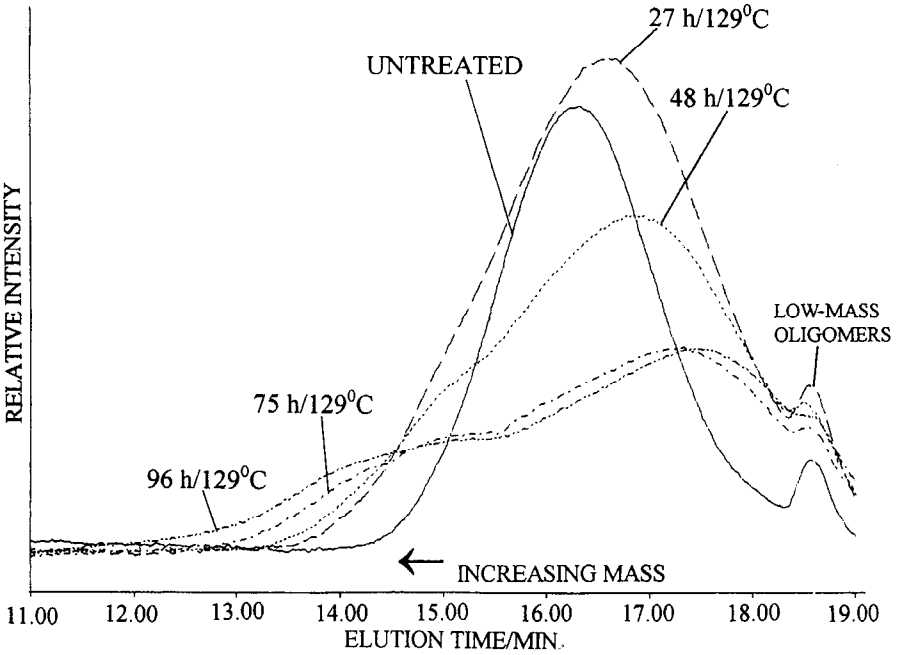

Fig. 1. SEC chromatograms of polynimmo both untreated (solid line) and pyrolysed for various times at 129°C (various broken lines).

2.6. N.m.r. spectroscopy

Our previous routines were followed using Bruker AC 250 and 400 spectrometers (all ^{13}C spectra were measured with the AC 400 machine).

3. Results and discussion

This section is divided into two parts: Part 1 deals with spectral characterization of polynimmo following pyrolysis without any attempt to separate what transpired to be a rather complex mixture of products. Part 2 covers characterization of pyrolysis products following exhaustive column chromatography.

3.1. Part 1. Spectral characterization of the pyrolysis of polynimmo by SEC

Polynimmo (4.0 g) was placed in a glass vial (20.0 cm^3) and pyrolysed in an oven at 130°C for up to 96 h. Samples (0.10 g) of the pyrolysate were removed after 27, 48, 75 and 96 h. The polymer becomes gradually more viscous, darker in colour and harder to dissolve as the heating time is increased.

Fig. 1 shows the SEC chromatograms for the pyrolysed samples and for untreated polynimmo obtained using the high molecular weight column system (see Experimental). Clearly pyrolysis has resulted in the formation of both lower and higher mass polymeric material, reflecting the occurrence both of chain scission and cross-linking. The nominal molecular weight of polynimmo decreases from its original value of approximately 5000 to a value of approximately 3000 Da after 96 h pyrolysis. A substantial amount of higher molecular weight material is also formed, presumably via a cross-linking process, and the weight average molecular weight increases from its original value of 9000 to 24 000 Da.

The low molecular weight column system gave more accurate results during the first 10 h of pyrolysis as the molecular weight changes of polynimmo are relatively small over this time period. SEC data show that during the first 3 h of pyrolysis at 130°C, chain scission occurs to produce lower molecular weight polymer, but no higher molecular weight material is evident. Thus, it appears that there is a minimum period before cross-linking reactions occur. If the rate of oxygen consumption exceeds the rate of oxygen permeation, as is often the case for solid polymers [14–16], oxidation occurs in the surface layers whereas the bulk core of the polymer remains practically unoxidized. Thus, at 130°C oxidation proceeds rapidly and the available oxygen is quickly used up. However, during the first few hours of pyrolysis at 130°C, the oxygen levels in polynimmo are relatively high. The thermal oxidation mechanism of polynimmo given below indicates that thermolysis results in chain scission. Presumably, in the presence of excess oxygen, the rate of oxidation and thus of chain scission is far greater than that of cross linking, but the importance of the latter increases as the oxygen supply becomes exhausted. The importance of this effect depends on several intrinsic parameters such as material geometry (e.g. sample thickness) coupled with oxygen consumption rate, which depends in turn on the reactivity of the polymer, the presence of additives and the oxygen permeability of the

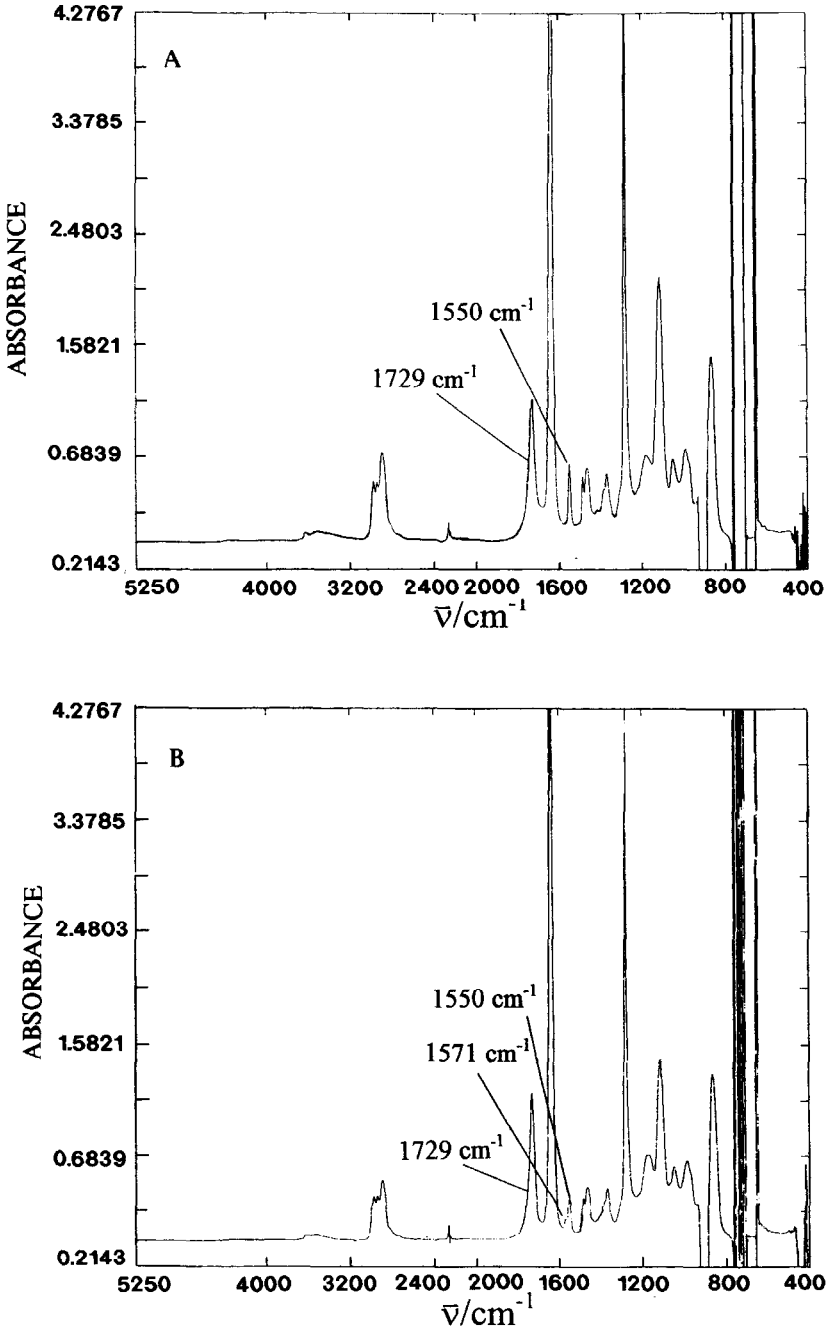

Fig. 2. Solution i.r. spectra of polynimmo following pyrolysis for 12 h at 145°C. (A) Pyrolysis in glass vial; (B) pyrolysis in thin layer on flat plate.

material [15,16]. Polynimmo was pyrolysed at temperatures varying between 90 and 150°C, but no significant differences in the distribution of lower and higher mass pyrolysis products were apparent in the SEC chromatograms.

3.1.1. Characterization of pyrolysed polynimmo by solution i.r. spectroscopy

Preliminary investigations into the oxidative process were performed using *FT*i.r. Polynimmo (5.0 g) was placed in glass vials (20.0 cm^3) and pyrolysed in the oven at 145°C. New absorptions became visible via solution i.r. at 1729 and 1550 cm^{-1}. Both peaks appear to increase in intensity at approximately the same rate over a 4 h pyrolysis. The absorption at 1729 cm^{-1} appears in the region for carbonyl compounds and is assigned to a carbonyl-containing product.

Similar experiments using thin films of polynimmo coated on glass plates were subsequently performed. Polynimmo was spread as thinly as possible on a glass plate (20 × 20 cm). A glass vial (20 cm^3) was filled with polynimmo (4.0 g) so that a depth of approximately 3 cm was achieved. Both the plate and vial were placed in the oven at

145°C and pyrolysed for a period of 12 h over which time samples were removed and analysed by solution i.r. spectroscopy. It was found that the relative intensities of the two i.r. absorptions at 1729 and 1550 cm^{-1} differed substantially between the two sample configurations, as summarised below.

(i) Glass vial geometry: over the first 4 h of pyrolysis the samples showed nearly identical intensities at 1729 and 1550 cm^{-1}. However, over the next 8 h of pyrolysis, the absorption at 1729 cm^{-1} became gradually more intense until it was approximately twice as intense as that at 1550 cm^{-1}.

(ii) Flat glass plate geometry: the most noticeable feature here is the *immediate* presence during the first 4 h of thermolysis of one absorption at 1550 cm^{-1} and another at 1571 cm^{-1}. The absorption at 1550 cm^{-1} increased in intensity at a slightly lesser rate than its counterpart in the glass vial experiment. However, the peak at 1729 cm^{-1} increased in intensity at a rate nearly double that of its counterpart.

Fig. 2(A), (B) shows the solution i.r. spectra ($CHCl_3$) obtained for the polynimmo samples from the glass vial and glass plate, respectively, after 12 h pyrolysis at 145°C. The glass plates were covered in very thin films of polymer and thus it became increasingly difficult to obtain equivalent masses of sample from the glass plate as only very small amounts of polymer could be removed from the plate. Consequently, the concentrations of the samples used to obtain the i.r. spectra in Fig. 2 were somewhat different.

These results can partly be explained by the limitation of diffusion of oxygen (see above). Thus, if the rate of oxygen consumption exceeds that of oxygen permeation, as it should do for the thicker sample (glass vial), then oxidation occurs in the surface layers while the core remains practically unoxidized. However, thinner samples should exhibit more rapid carbonyl growth as the surface area of the polymer is relatively larger. Lowering the pyrolysis temperature enhances the relative growth of the 1729 cm^{-1} peak as there is more time for oxygen diffusion to occur. The increased oxygen diffusion at lower temperature also results in the production of a complex mixture of secondary oxidation products absorbing from 1700–1800 cm^{-1}.

The absorption at 1550 cm^{-1} increased in intensity at a slightly lesser rate for the sample on the glass plate. Separate experiments comparing even thinner films to even thicker samples of polymer showed that this effect became even more pronounced. The absorption at 1550 cm^{-1} could be due to a number of different species. Candidate species include carboxylate, alkene, nitro, nitroso and nitrite compounds. If one of the latter three species is associated with the new absorption, its formation may be expected to result from the loss and subsequent reaction of NO_x. If this process were reduced in significance, i.e. if NO_x were lost to the atmosphere without reacting, then a lower concentration of product would be expected. An attempt was made to induce this effect in polynimmo by pyrolysing a *thin* film; as the surface area is increased and the film thickness decreased, relatively more NO_x should be lost without reacting, thus decreasing the amount of product resulting from the polymer's reaction with NO_x. As this was borne out by experiment, it appears likely that the absorption at 1550 cm^{-1} results from the reaction of polynimmo with NO_x and at this stage we tentatively assigned this band to the asymmetric stretching frequency in a nitroalkane. In shape, position and intensity the band at 1550 cm^{-1} strongly resembles those found in nitrobenzene [17], *t*-nitrocyclohexane [18] and many other nitroalkanes [18,19].

Comparison of the i.r. spectra of untreated and pyrolysed polynimmo shows that there is an increase in intensity of the bands in the region around 1000 cm^{-1}. Consequently, i.r. difference spectra of the pyrolysed polynimmo samples obtained from the glass vial/flat plate experiments were run. Fig. 3 shows the i.r. difference spectrum obtained by subtracting the spectrum for untreated polynimmo from that for pyrolysed polynimmo (6 h/145°C): both spectra were run using identical concentrations of polynimmo. The absorptions at 1729 and 1550 cm^{-1} are clearly visible. Other new absorptions at 3500, 1170, 1085, 1050 and around 1400 cm^{-1} are also visible. The band around 3500 cm^{-1} appears to consist of a sharp unbonded hydroxyl band at 3526 cm^{-1} and a broad bonded hydroxyl band around 3400 cm^{-1}. The absorption around 1170 cm^{-1} appears broad and may consist of multiple absorptions. Many different carbonyl species absorb in this region but the absorption frequency of the carbonyl group (1729 cm^{-1}) suggests that these absorptions may belong to the stretching and bending vibrations of the C–C(=O)–C group in ketone compounds or the stretching vibrations of the C–O group in ester compounds. The absorptions around 1085 and 1050 cm^{-1} are consistent with the stretching vibrations of the C–O group of esters and alcohols.

3.1.2. Characterization of pyrolysed polynimmo by ^1H and ^{13}C n.m.r. spectroscopy

^1H and ^{13}C n.m.r. spectra of the pyrolysed samples from the glass vial and glass plate experiments described above were recorded. As with i.r. spectra, the n.m.r. spectra of the polynimmo samples obtained from the glass plate and vial differed only in their relative peak intensities. Fig. 4(A) and (B) shows the ^1H and ^{13}C n.m.r. spectra, respectively, of pyrolysed polynimmo which was obtained from the glass vial after 12 h pyrolysis at 145°C. The peaks due to the original methyl and methylene protons have broadened considerably due to the increased viscosity and thus lowered mobility of the pyrolysed polymer. Many new resonances are visible around 4.0 ppm, making assignments difficult. Accordingly, column chromatography was employed to separate this complex mixture of pyrolysis products and these peaks are assigned below. Two new resonances were observed at low field. The most readily formed of these appears at $\delta_H = 8.09$ ppm and is visible after 5 min at 145°C, while the second appears at $\delta_H = 9.53$ ppm and can be seen after 10 min at 145°C. The peak at 9.53 ppm

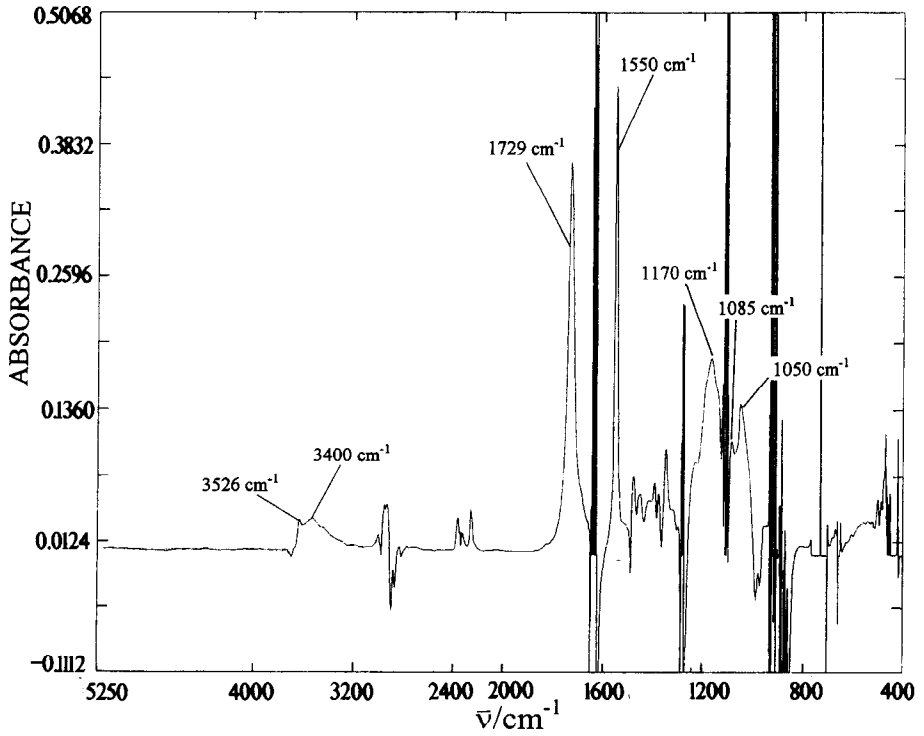

Fig. 3. I.r. difference spectrum obtained by subtracting the spectrum of untreated polynimmo from that of polynimmo pyrolysed for 6 h at 145°C.

increases in intensity over the first 4 h of pyrolysis and then remains at constant, but very low intensity; it is only visible when the spectrum is enlarged (see inset to Fig. 4(A)). The peak at 8.09 ppm continues to increase in intensity over the course of the pyrolysis. Similarly, a small but sharp new peak at $\delta_H = 2.1$ ppm increases in intensity during pyrolysis which resembles that reported in the thermal degradation of poly(propylene oxide) (PPO) [20]. PPO has many structural similarities to polynimmo and its degradation products have been characterized by ^{1}H n.m.r. [20], thus a peak at $\delta_H = 2.1$ ppm is visible in the ^{1}H n.m.r. spectrum of PPO on pyrolysis which is assigned to a methyl group attached to a carbonyl carbon in a ketone. Accordingly, this minor species may also be attributed to a methyl ketone.

New peaks are visible at $\delta_c = 160.3$ ppm and 89.4 ppm in the ^{13}C n.m.r. spectrum (Fig. 4(B)) of pyrolysed polynimmo (the latter peak is assigned below). Carbonyl formation has already been demonstrated by i.r. spectroscopy, and in the absence of any other new peaks in this region, the peak at $\delta_c = 160.3$ ppm is assigned to a carbonyl group. Due to its field position, this resonance is most probably associated with an ester as opposed to a ketone which would give a resonance at lower field. Two-dimensional n.m.r. was employed to ascertain whether this resonance is associated with the peak at $\delta_H = 8.09$ ppm in the ^{1}H n.m.r. spectrum.

A two-dimensional ^{1}J^{1}H–^{13}C correlation experiment (see Fig. 5) showed that the proton associated with the resonance at $\delta_H = 8.09$ ppm *is* directly attached to the carbonyl group associated with the resonance around $\delta_c = 160.3$ ppm in the ^{13}C n.m.r. Consequently, the most likely assignment of the carbonyl group is to a formate ester. The position of the carbonyl absorption around 1729 cm^{-1} in the i.r. spectrum of pyrolysed polynimmo also closely matches the carbonyl absorptions of ethyl, *n*-propyl and *n*-butyl formate which absorb around 1725 cm^{-1} [21,22]. Pyrolysis experiments were also performed using degassed solutions of polynimmo sealed under dynamic vacuum. The rates of development of the absorbance at 1729 cm^{-1} in the i.r. spectrum and the associated resonance at $\delta_H = 8.09$ ppm in the ^{1}H n.m.r. were significantly reduced as compared with those of samples of polynimmo pyrolysed in air, thus substantiating our assignment of the carbonyl compound as an autoxidation product. Exhaustive attempts to inhibit completely carbonyl development were unsuccessful. Indeed, carbonyl development became increasingly difficult to inhibit with increasing concentration of the polynimmo solution due to the difficulty in degassing more viscous solutions. It is, of course, quite possible that certain of the products of decomposition (see below), such as NO_2, can induce carbonyl formation.

Other new resonances are also visible around 66.0 and 71.0 ppm in the ^{13}C n.m.r. spectrum of pyrolysed polynimmo. Clearly these new resonances are complex and consist of many peaks, making the assignment of individual peaks very difficult. However resonances around 60–80 ppm in the ^{13}C n.m.r. spectrum are often associated with alcohols and ethers formed during the thermal degradation of polymers [23], the latter as a result of combination of alkyl and alkoxyl radicals. The mechanism (Scheme 1) shows the proposed oxidation leading to production of the

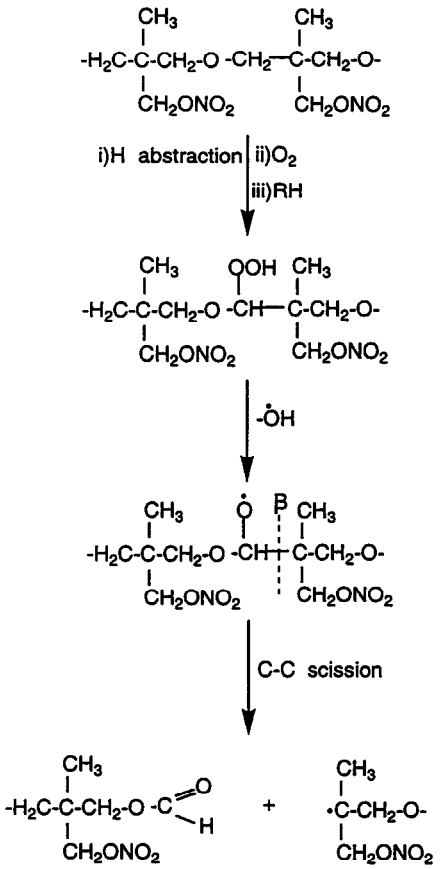

Scheme 1. Proposed mechanism for the formation of the formate ester during pyrolysis of polynimmo.

formate ester. We propose that the tertiary, secondary and primary carbon-centred radicals generated during the thermal degradation of polynimmo may lead to the formation of alcohol species via alkoxy radicals.

Clearly the formate ester can be produced by hydroperoxide formation at either of the methylene groups in polynimmo, although there is probably a parallel pathway involving the oxidation of formaldehyde to formic acid which then esterifies alcohol products. The resulting alkoxy radical appears to undergo predominantly C–C bond cleavage (β scission), as observed in poly(ethylene oxide) and PPO. However, low intensity peaks around 9.5 ppm, indicative of an aldehyde species, are also observed in the ^{1}H n.m.r. spectrum of pyrolysed polynimmo.

The tertiary carbon-centred radical generated in the mechanism shown above may react similarly to the secondary polymer radical to form an alkoxy radical. The alkoxy radical may then undergo a similar β scission or it may abstract hydrogen from another polymer chain to give a tertiary alcohol. Clearly a secondary alcohol will also be formed if the secondary alkoxy radical shown in the scheme above similarly abstracts hydrogen. Any attempt to devise oxidation mechanisms beyond the initial stages of degradation would be speculative, but it is clear that various species of alcohol exhibiting resonances around 60–80 ppm in the ^{13}C n.m.r. spectrum may be produced during the thermal degradation of polynimmo.

Due to the lower mobility of the pyrolysed polymer, long scan times were required to obtain well-resolved ^{13}C n.m.r. spectra. It was found that far greater spectral resolution was observed when spectra were recorded above room temperature. Consequently, and to avoid any solvent effects, spectra were recorded using neat polynimmo before and after pyrolysis. Due to the gradually increasing viscosity of the polymer with longer pyrolysis times, there exists a limit where the resonances in the ^{13}C n.m.r. spectra become so broad and poorly defined that continued analysis is futile. This seems to occur after approximately 45 h pyrolysis at 145°C in a 10 mm n.m.r. tube. Fig. 6 shows the ^{13}C n.m.r. spectrum obtained at 90°C for pyrolysed polynimmo (45 h/145°C). Various new resonances, not previously visible in the solution spectra, appear in the region between 100 and 220 ppm, to which only very general attributions can be given. New resonances around 205 ppm are most probably associated with aldehyde or ketone species. Resonances around 175 ppm are characteristic of ester species produced by direct oxidation at the methylene carbons in the main chain of polynimmo; thus in the absence of chain scission, carbonyl formation will result in an ester. Resonances around 100–150 ppm are characteristic of alkenes.

3.1.3. Characterization of pyrolysed polynimmo by e.s.r.

Polynimmo (0.5 g) was placed in quartz pipette tubes and heated in the oven at temperatures between 100° and 155°C. Preliminary investigations led to the detection of a very clearly defined paramagnetic species. Fig. 7 shows the e.s.r. spectrum of pyrolysed polynimmo (5 h/150°C) measured at room temperature. Identical spectra were also obtained from the pyrolysis of degassed samples of polynimmo sealed under dynamic vacuum and from the pyrolysis and photolysis of both cured and uncured polynimmo samples in air. Heating over various lengths of time produces a gradually increasing concentration of this odd-electron species which remains stable over a period of months. Few such radicals are stable over this time scale; candidate molecules are the nitroxyls, nitrogen dioxide and trapped polymer peroxyl radicals. The exact anisotropic g-tensors were extracted from the spectra and are shown on the spectrum in Fig. 7.

As high a concentration of the radical species obtained by heating could not be achieved by photolysis, but the g-tensors of the species generated by either method are nearly identical. Samples of polynimmo heated under vacuum and in air gave similarly intense spectra, indicating that oxygen is not a requirement for this free radical formation. Consequently peroxyl formation seemed unlikely as anaerobic conditions would presumably lead to a lower rate of radical formation. Nitrogen dioxide, being paramagnetic and a known product of thermolysis of nitrate esters, seemed a possible attribution to the unknown radical. However, the spectral shape and g-tensors of the unknown radical in

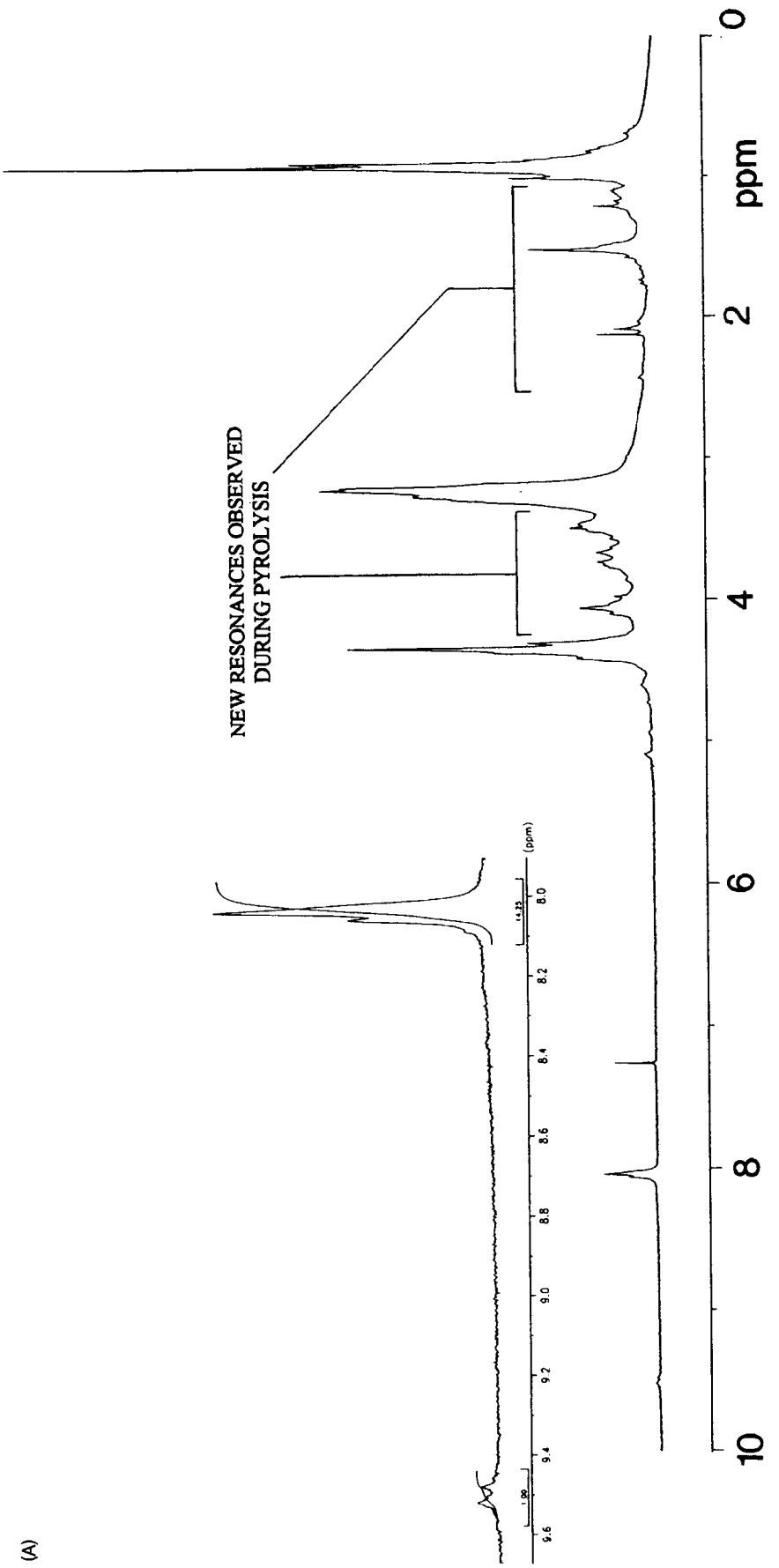
NEW RESONANCES OBSERVED
DURING PYROLYSIS
ppm
0
2
4
6
8
10
(ppm)
8.0
8.2
8.4
8.6
8.8
9.0
9.2
9.4
9.6
1.00
1.425

(A)

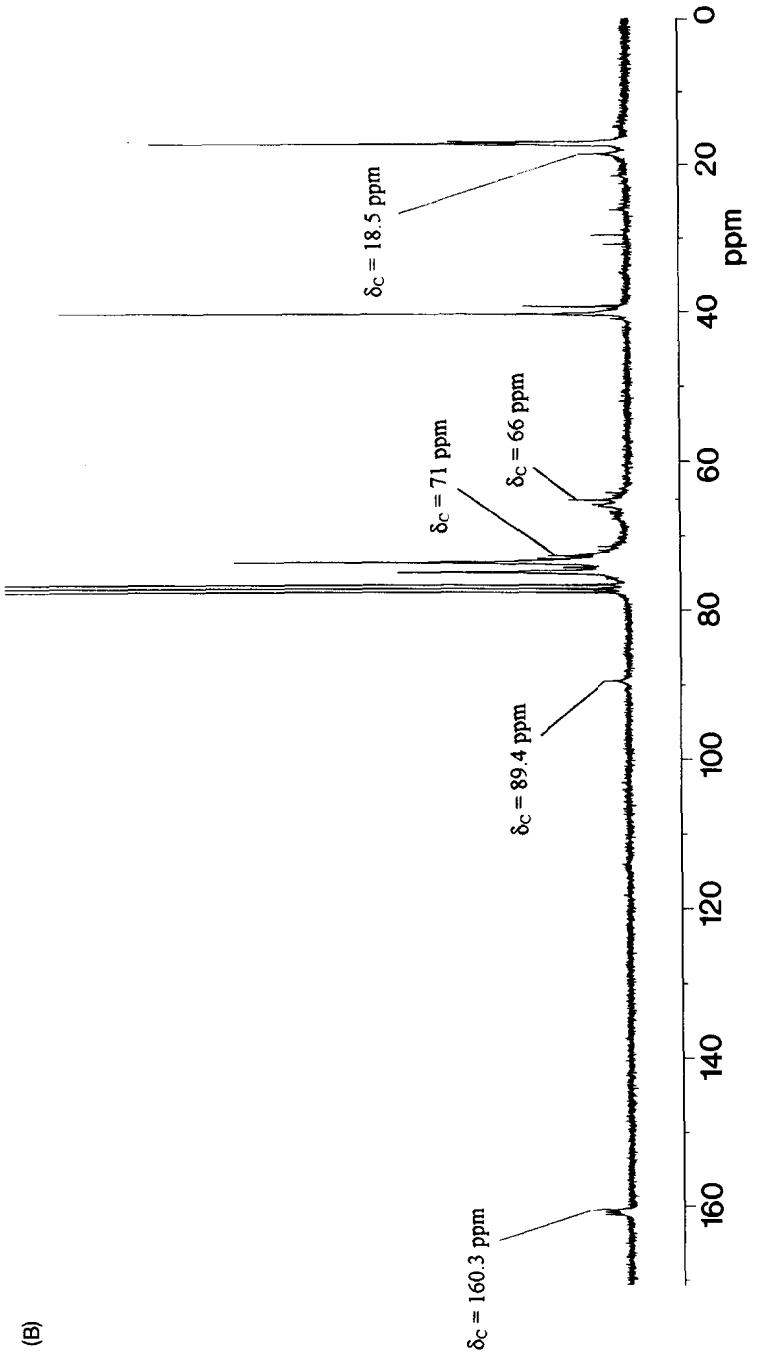

Fig. 4. N.m.r. spectra of neat polynimmo pyrolysed for 12 h at 145°C. (A) 250 MHz ^{1}H spectrum; (B) ^{13}C spectrum run on AC 400 spectrometer.

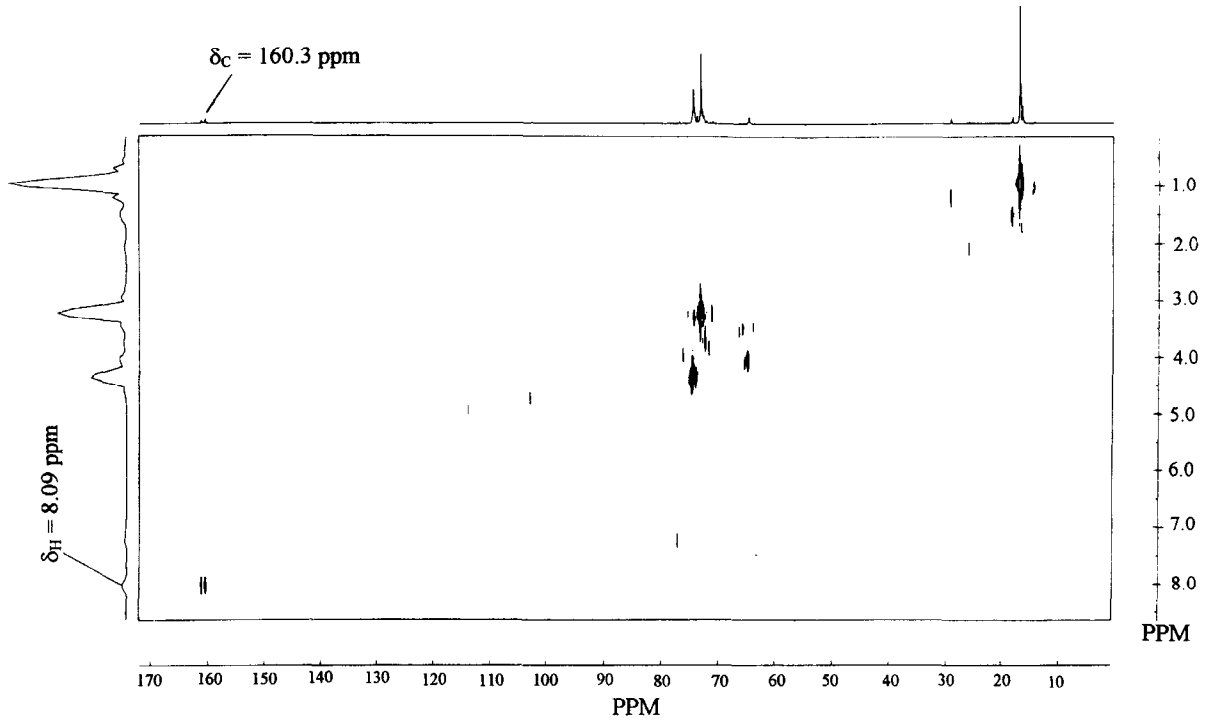

Fig. 5. Two-dimensional (^{1}J,^{1}H–^{13}C correlation) n.m.r. spectrum of polynimmo pyrolysed for 12 h at 145°C run on AC 400 spectrometer.

pyrolysed polynimmo are substantially different from those observed for NO_2 in various media [24–29].

A recent paper by Chen et al. [30] describes the use of paramagnetic labels to study the motional processes and phase transitions in polyurethanes. The paper describes the application of the nitroxide probe, 4-hydroxy-2, 2′, 6, 6′-tetramethylpiperidine-1-oxyl (TEMPOL). This probe, once attached to the polyurethane, displays ESR spectra virtually identical to those obtained for our unknown. Chen et al. do not give *g*-tensor values, but the width of their radical measured in gauss (G) and its shape at 120 K are nearly identical to that of the species produced from polynimmo. The *g*-tensor values for the radical produced from pyrolysis of polynimmo also very closely match those for many other nitroxides [31] and consequently, it is assigned to a nitroxide. To confirm this assignment, a sample of TEMPOL was dissolved into untreated polynimmo using chloroform as a solvent (10 mg TEMPOL/g of polynimmo). The spectral shape of the resulting TEMPOL radical was found to differ according to the concentration of the solution added to polynimmo. Thus, the addition of 0.5 cm^3 of chloroform containing 10 mg of TEMPOL, to 1 g of polynimmo produced a spectral shape that mimics that of TEMPOL at 260 K, while the addition of less concentrated solutions produced a spectral shape that mimics that at 300 K. Therefore, it appears that the spectra resulting from the increased mobility of the TEMPOL radical due to the addition of solvent or increased temperature are nearly

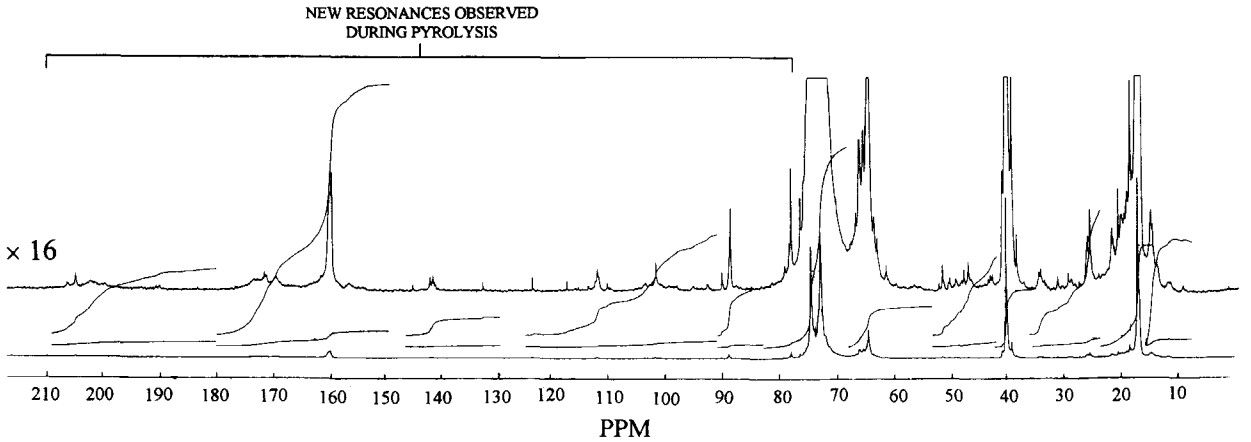

Fig. 6. High field ^{13}C n.m.r. spectrum of polynimmo pyrolysed at 145°C for 45 h (measured at 90°C).

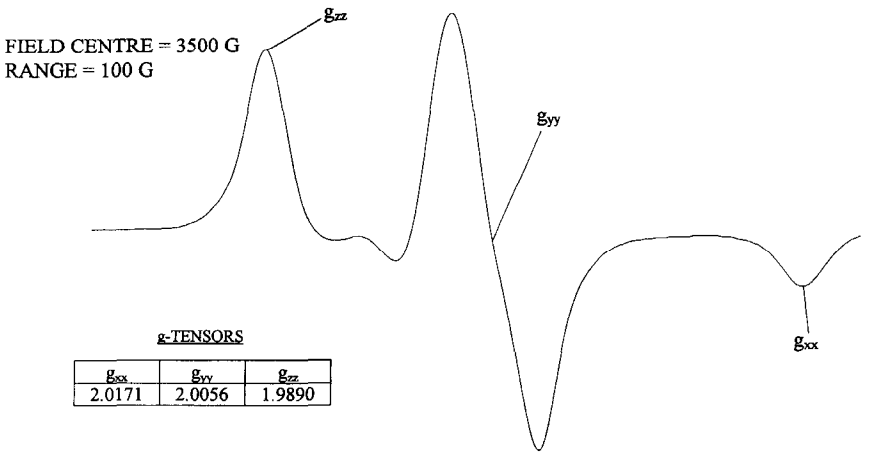

Fig. 7. Room-temperature ESR spectrum of polynimmo pyrolysed for 5 h at 150°C.

identical. Consequently, the spectrum of the radical attributed to a nitroxide in pyrolysed polynimmo was expected to change in shape similarly. The ESR spectrometer used in our study was not equipped with a variable temperature cavity, but the increased mobility of the radical can be mimicked by addition of solvent to pyrolysed polynimmo. Fig. 8(B) shows the ESR spectrum of pyrolysed polynimmo (5 h/150°C) after the addition of 0.5 cm^3 of chloroform, measured at room temperature. As expected, due to the increased mobility of the radical, this spectrum more closely resembles the spectrum obtained for TEMPOL at elevated temperature (260 K).

Fig. 8 shows the ESR spectrum of pyrolysed polynimmo after 15 min pyrolysis at 150°C. Clearly, this spectrum differs from that obtained at longer pyrolysis time (Fig. 7) in the relative intensity of the peak denoted by the asterisk. The literature ESR spectra of the TEMPOL-labelled polyurethane show that this same peak appears to increase in intensity on warming from 120 to 200 K and further increases in intensity to become the principal line in the spectrum at 260 K. Thus, the relatively greater intensity of this peak in the spectrum of polynimmo after shorter pyrolysis times (Fig. 8(A)) as compared with longer pyrolysis times (Fig. 7) is attributed to the increase in viscosity and thus reduced mobility of the polymer with increasing pyrolysis times.

Thus, the changes in spectral shape brought about by the differing mobility of the radical produced during pyrolysis of polynimmo exactly mimic those observed for the nitroxide probe TEMPOL. This supports our assignment of the paramagnetic species in pyrolysed polynimmo to a nitroxide. The first report of a nitroxide radical produced in a nitrate ester polymer during degradation was made in a communication by Yamauchi et al. [32] in 1993 during the course of our work. These spectra, produced during the photoirradiation of cellulose nitrate films, are complicated by the presence of alkylperoxyl and alkoxyl radicals not detected in polynimmo; the presence of two different nitroxide radicals further complicates this spectrum. The proposed mechanism of formation of one of these nitroxide radicals during photolysis of cellulose nitrate, shown below, is thought to be the same as that for the nitroxide radical produced during photolysis or pyrolysis of polynimmo. Thus, NO or NO_2 evolved during photo or thermal degradation of polynimmo may react with alkyl radicals, producing nitroso or nitro compounds which have no unpaired electron. These molecules may then trap other alkyl radicals

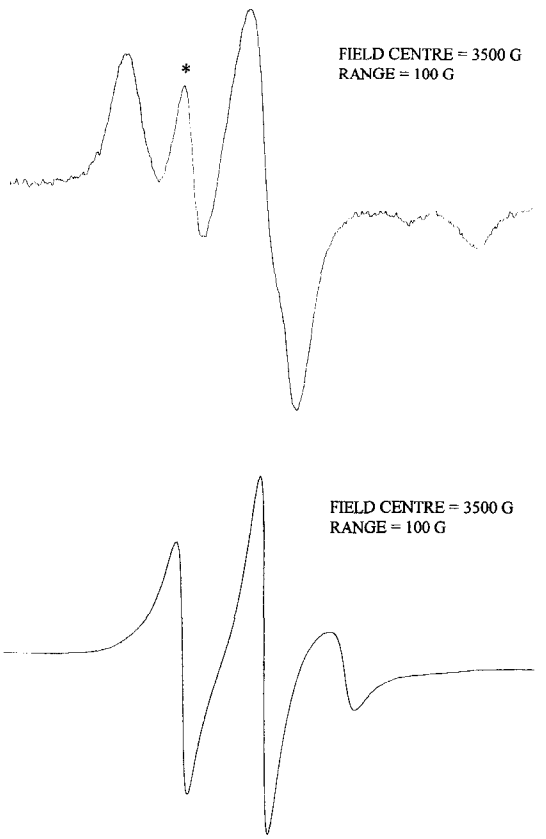

Fig. 8. ESR spectrum of pyrolysed polynimmo. (A) pyrolysis time 15 min at 150°C, measured at 298 K as neat polynimmo. (B) pyrolysis time 5 h at 150°C, measured at 298 K in $CHCl_3$.

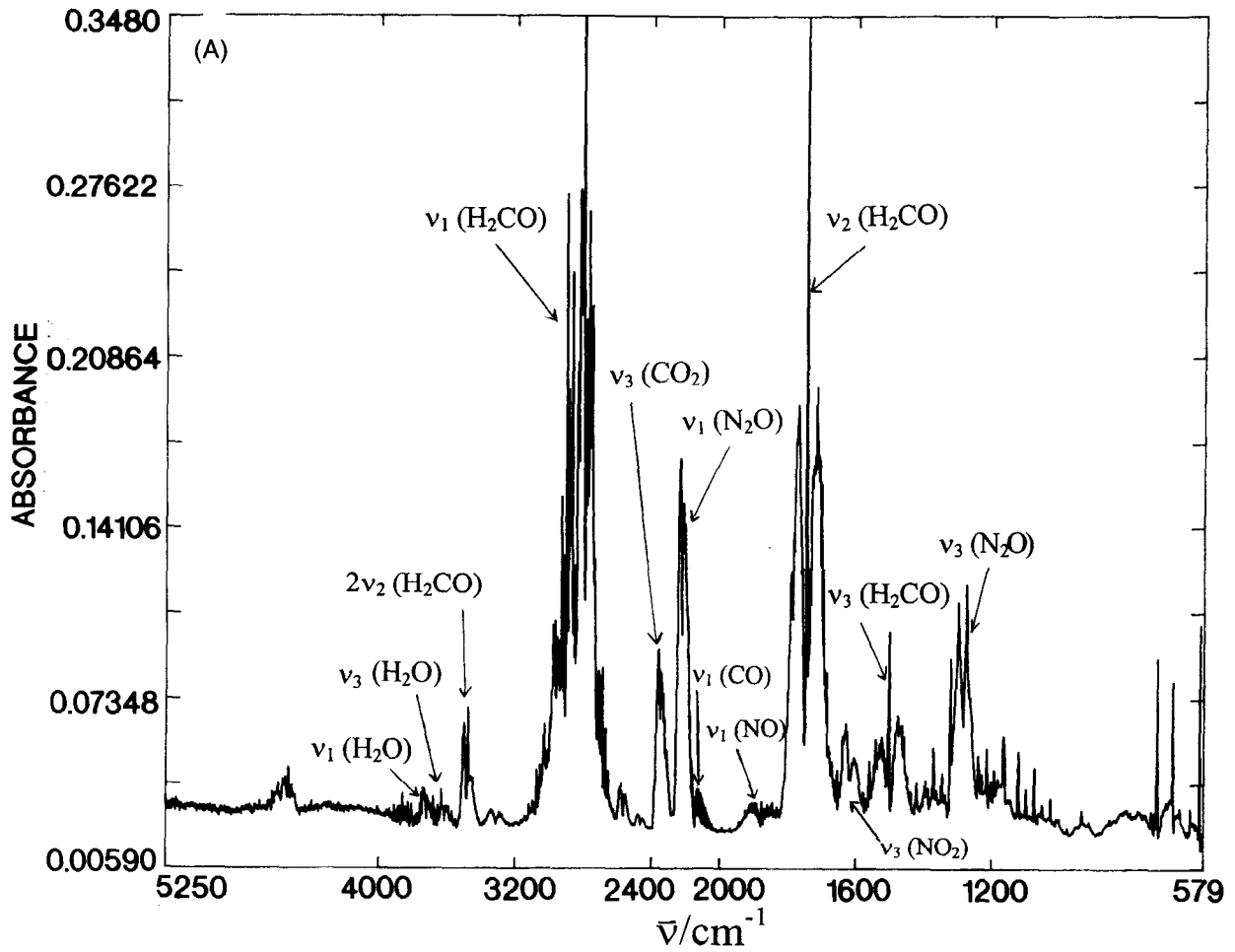

Fig. 9. (A) Gas-phase i.r. spectrum of gases evolved on pyrolysis of polynimmo for 15 min at 155°C. (B) Gas-phase i.r. spectrum of gas sublimed from white solid residue (see following page).

in a type of spin-trapping process, resulting in nitroxide radicals:

$$R^{\cdot} + NO \rightarrow R\text{–}NO \xrightarrow{R'^{\cdot}} RR'NO^{\cdot} \quad (1)$$

$$R^{\cdot} + NO_2 \rightarrow R\text{–}NO_2 \xrightarrow{R'^{\cdot}} R\text{–}N(\text{–}O\cdot)\text{–}OR' \quad (2)$$

The formation of a nitroalkane during pyrolysis of polynimmo is shown below and thus the mechanism in Eq. (2) appears a likely path to the formation of the nitroxide. Although nitroso species are not detected in the n.m.r., i.r.(solution) or ESI (below) spectra during pyrolysis of polynimmo, the mechanism in Eq. (1) cannot be completely excluded; nitroso species formed during pyrolysis of polynimmo may not be detected due to their rapid reaction rates with alkyl radicals.

Ranby [33] reports that most polymers show asymmetric singlet spectra attributed to ROO$^{\cdot}$(RO$^{\cdot}$) radicals, which are generated after the exposure of samples containing R$^{\cdot}$ to air. However exhaustive attempts by us to trap alkylperoxy or alkoxy radicals at either 77 K or at room temperature using spin traps were unsuccessful. We attribute this to the experimental conditions employed by us, as clearly alkoxy and alkylperoxy radicals are observed in a wide range of polymers, such as polyethylene and polypropylene, during irradiation [33].

3.1.4. Characterization of pyrolysis gases from polynimmo by gas phase i.r. spectroscopy

Many studies have been conducted on the i.r. and mass spectrometric analysis of gases evolved from heated samples of various propellant formulations [9,34]. However, all of these studies have employed rapid heating rates in the range 100–200 K s^{-1} in an attempt to simulate macroscale combustion behaviour. The kinetics of weight loss during programmed heating at 150°C/s have been determined by simultaneous mass and temperature change (SMATCH)/*FT*i.r. spectroscopy for polynimmo [8] and other structurally similar propellants [35]. However, in our study of polynimmo, its relatively slow thermal decomposition is monitored at constant temperature in the range 70–155°C. At lower temperatures, processes with lower activation energies and greater exothermicity are favoured, while conversely, at higher temperatures, the higher activation

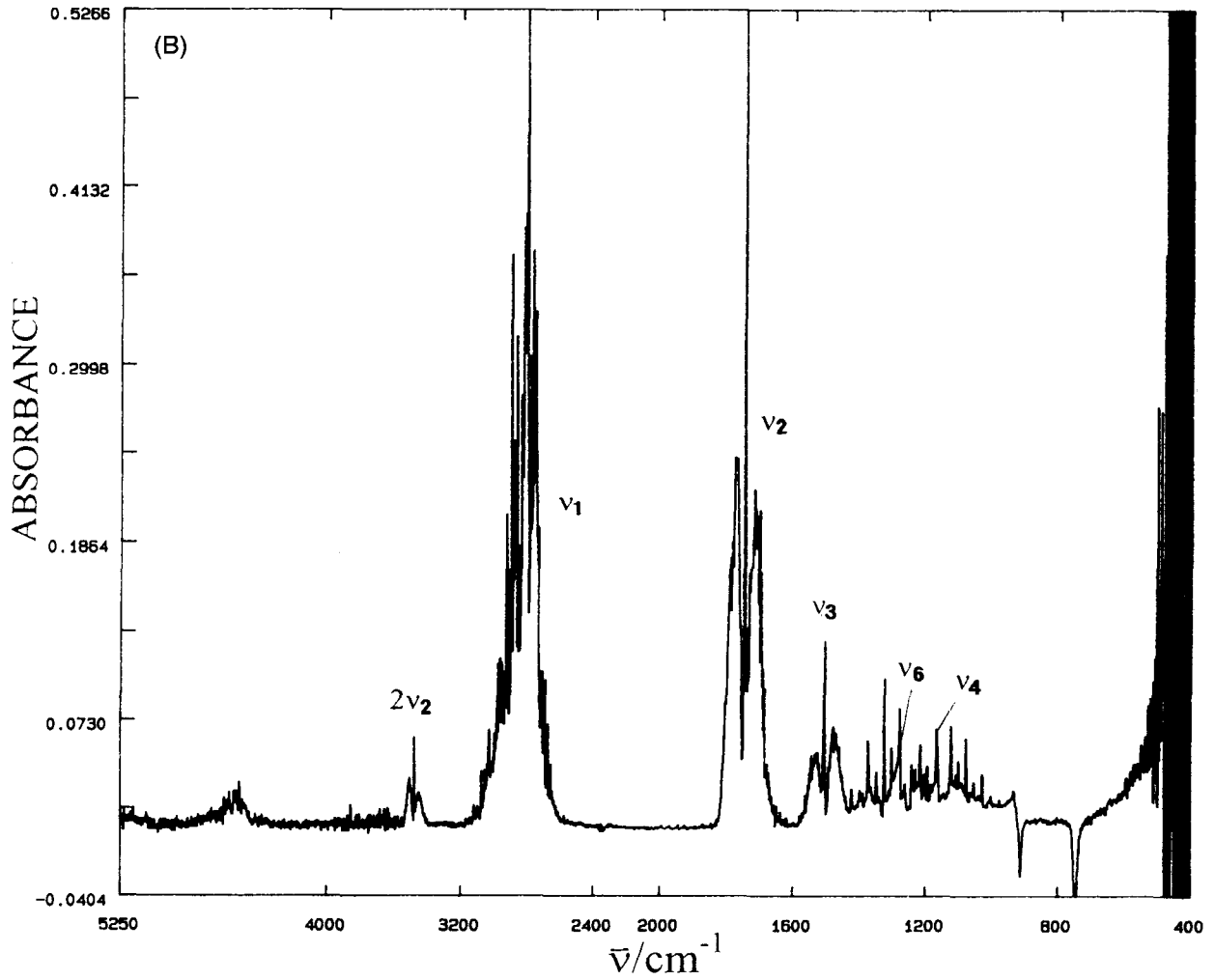

Fig. 9. (*continued*) For legend see previous page.

energy and more endothermic processes become predominant. However, the products have a shorter time to form and may or may not be the same as products formed at lower temperature. Consequently, descriptions of decomposition processes depend significantly on the temperature and the heating rate.

Experiments were performed according to the method given in the Experimental section. Polynimmo was heated at temperatures in the range 70–155°C using an oil bath, and the pyrolysis gases were collected in a i.r. gas cell and characterized by i.r. spectroscopy. Preliminary experiments to separate and quantify the relative amounts of pyrolysis gases were performed using gas chromatography. However the chromatograms obtained were unreproducible and this was most likely attributed to our experimental procedure. GC/MS experiments were also performed; polynimmo samples were heated at 155°C in an oil bath and the gases were analysed via GC/MS using an MS80 mass spectrometer. We were unsuccessful in separating the gases, but individual gases could be identified by their ion peaks in the mass spectrum. Thus the relative amounts of individual gases are not accurately known. However, the relative intensities of the peaks in the i.r. spectrum give an approximate idea of the relative amounts of pyrolysis gases present.

Fig. 9 shows the gas phase i.r. spectrum of the pyrolysis gases obtained by heating polynimmo for 15 min at 155°C. The peak assignments shown on the i.r. spectrum are based on high purity standards [36–39]. Infrared-inactive species H_2, N_2 and O_2 may also be present and, indeed, in separate experiments run at similar pyrolysis temperatures, significant quantities of both N_2 and O_2 were detected in the electron impact (EI) mass spectrum of the pyrolysis gases; the observation of N_2 is particularly interesting as it implies extensive reduction of NO_x species in the overall process.

If the sealed i.r. cell was left at room temperature for approximately 30 min after collecting the pyrolysis gases, a considerable amount of white solid became visible on the inside of the cell. The cell was re-evacuated and warmed with a hair drier. The white solid sublimed and the i.r. spectrum of the resulting gas was recorded (see Fig. 10(B)). The peaks in this spectrum exactly match those expected for

formaldehyde. The fundamental frequencies υ_1, υ_2 and υ_3, and the first overtone of the υ_2 frequency are clearly visible in this spectrum and in Fig. 9(A). Presumably, the original white solid is paraformaldehyde.

The relative intensities of the peaks in the gas-phase i.r. spectrum of pyrolysed polynimmo, and thus the gas composition, appear to vary only in the relative amounts of nitrogen-containing species as compared to formaldehyde present. The peaks due to formaldehyde are similarly or less intense than the peaks due to the nitrogen-containing species when the pyrolysis temperature is less than 120°C. As the pyrolysis temperature is increased, the formaldehyde peaks gradually become increasingly more intense as compared to the nitrogen-containing species. Pyrolysis temperatures in excess of 140°C produce gradually increasing concentrations of nitrogen-containing species although the formaldehyde peaks remain more intense (see Fig. 9(A)). The peaks due to NO_2(g) are only visible in the spectra recorded above 150°C. NO_2(g) gives strong bands [40] in the i.r. but, even with pyrolysis temperatures of 155°C, the intensity of the peaks due to NO_2(g) is very low. This seems curious if we consider that the first step in the thermal decomposition of nitrate esters is generally thought to be the reversible homolysis of the O–NO_2 group [8,10].

$$RONO_2 \rightleftarrows RO^{\cdot} + NO_2^{\cdot} \quad (3)$$

The presence of NO_2 was confirmed by ion peaks at 46, 30 and 16 Da in the EI mass spectrum of the pyrolysis gases of polynimmo, although, as for the gas phase i.r. spectrum, these peaks were relatively weak. Various explanations for the relatively low concentration of NO_2(g) are possible. The first is a result of the effect shown above, i.e. NO_2(g) has a relatively greater chance of reacting with the polymer during pyrolysis of thick films as compared to thin films of polynimmo. Except when Eq. (1) occurs on the surface, the NO_2(g) must migrate through the polymer matrix. The absorption at 1550 cm^{-1} in the solution i.r. spectra of pyrolysed polynimmo, due to the reaction of polynimmo with NO_x(g) and later identified as a nitro species (see below), is relatively more intense for thicker films as compared with thinner films of polynimmo. The intensity of the 1550 cm^{-1} absorption is approximately the same for samples of polynimmo pyrolysed at reduced pressure and polynimmo samples pyrolysed for similar amounts of time and at similar temperatures in air. Thus, because of the high reactivity of NO_2(g) at elevated temperatures, it is not surprising that much of the nitrogen appears as N_2O(g) and NO(g). Pyrolysis temperatures in excess of 140°C generate high concentrations of NO_x(g). Consequently, the lower viscosity of the polymer at higher temperature and thus the higher rate of diffusion of NO_x(g) through the polymer matrix results in a greater concentration of nitrogen-containing species being detected. N_2O(g) has been detected during the rapid heating of various nitrate ester polymers [9], but no mechanism for its formation appears to be given. We propose the following mechanisms (see Ref. [41] for Eq. (6):

$$2NO_2 \rightleftarrows N_2O_4 \quad (4)$$

$$2N_2O_4 \rightarrow 2N_2O + 3O_2 \quad (5)$$

or

$$2HNO \rightarrow N_2O + H_2O \quad (6)$$

It might have been expected that reduced pressure would affect the relative concentration of nitro species produced (1550 cm^{-1}) during pyrolysis of polynimmo. However, the relatively high stability of the nitrogen dioxide radical, coupled with the relatively long diffusion times through the viscous polymer matrix, suggest that very little difference is actually to be expected.

Reactions of NO_2(g) with other pyrolysis gases could also account for discrepancies in the relative concentrations of gases observed as it is clear that the increased diffusion rate may compete with an increased reaction rate due to the elevated temperature. These reactions are the subject of much controversy in the field of propellant combustion chemistry. Various mechanisms have been proposed for the reactions of the pyrolysis gases, which are thought to occur both under high and low pressure depending on the reactivity of the gases produced. In this respect, various energetic polymers have been grouped according to the extent of condensed phase reaction that occurs before gaseous products are detected [9,42]. Polynimmo is grouped at the top of this list of some 30 polymers and it is reported that its decomposition is dominated by intrinsic condensed-phase chemistry independent of the pressure in the range 1–1000 psi. Irrespective of whether the pyrolysis gases react in the condensed phase, some reaction may be expected to occur when the i.r. gas cell is warmed to room temperature. The reactions below have been suggested to account for the low concentration of NO_2(g) in the pyrolysis gases of octahydro-1, 3, 5, 7-tetranitro-1, 3, 5, 7-tetrazocine (HMX), cyclotriethylenetrinitramine (RDX) [43] and various nitrate ester polymers [8], although it is difficult to assess the extent to which these reactions occur for polynimmo.

$$2NO_2 \rightleftarrows 2NO + O_2 \quad (7)$$

$$7NO_2 + 5CH_2O \rightarrow 7NO + 2CO_2 + 3CO + 5H_2O \quad (8)$$

Nitro-nitrito isomerization has long been known to take place at an aliphatic carbon atom [44]. Isomerization of this kind has been cited as evidence for the low concentrations of NO_2(g) and larger quantities of NO(g) evolved from aliphatic nitro-substituted propellants [45]. Isomerization of this type is not expected for nitrate esters due to the low stability of the O–O bond, but it will occur for the newly formed nitro species absorbing at 1550 cm^{-1} in the solution i.r. spectra of pyrolysed polynimmo. Thus, the small amounts of NO(g) in the i.r. spectrum (Fig. 9(A)) may result from the thermal decomposition of this nitro species.

It is clear from the structure of polynimmo that formaldehyde may result from the decomposition either of the nitrate ester side chains or the main chain. Loss of $NO_2^{\cdot}$ from the side chain results in the formation of a highly reactive alkoxy radical which may eliminate formaldehyde to produce the more stable tertiary carbon-centred radical. Similarly, if chain scission occurs at the ether linkages along the polynimmo backbone (see below), an alkoxy radical is generated which may undergo the same elimination process.

SMATCH/*FT*i.r. data for polynimmo [8] and poly(vinyl nitrate) (PVN) [8], which possesses no primary alkyl nitrate sites, shows that formaldehyde is still detected in the combustion products of PVN, although to a lesser extent than for polynimmo. Similarly 3-azidomethyl-3-methyloxetane (AMMO), which differs from polynimmo only in that it contains an azide side-group as opposed to a nitrate ester side group, also generates significant amounts of formaldehyde during rapid heating [8] (150 K s^{-1}). The fact that formaldehyde forms at all from PVN or AMMO indicates that it is not solely produced at these primary alkyl nitrate sites. Our SEC data for pyrolysed polynimmo shows that a considerable amount of chain scission is occurring during pyrolysis, but it is impossible to calculate the relative amounts of formaldehyde produced by the main chain and the side chains.

3.1.5. Characterization of pyrolysed polynimmo by ESI

Polynimmo (4.0 g) was placed in a glass vial (20.0 cm^3) and pyrolysed in the oven at 130°C for up to 60 h and samples were removed over various periods of time and analysed using ESI. Fig. 10 shows the ESI spectra of pyrolysed (48 h/130°C) and untreated polynimmo run at a cone voltage (cv) of 50. Clearly, the thermal degradation of polynimmo has resulted in a highly complex mixture of low-mass oligomers; there are considerably more peaks in the spectrum of degraded polynimmo as compared with untreated polynimmo, thus making the assignment of individual species very difficult. However, the spectra clearly show that the most intense ion peaks in the spectrum of degraded polynimmo are visible at 607.0 + 147*n* Da. We have previously assigned this series of ions to the H^+ adducts of the hydroxy-terminated linear oligomers [4]. Other peaks in the spectrum are similarly attributable to the undegraded linear oligomers [4]. The spectrum of untreated polynimmo shows that the most intense ion peaks are attributed to the cyclic oligomers with masses 606.0 + 147*n* [4]. Thus, it appears that the thermal degradation of polynimmo has resulted in an increased concentration of low-mass linear oligomers as compared to cyclic oligomers. The greater thermal lability of the latter can most likely be attributed to the strain in the cyclic oligomer ring as compared to its linear homologue. The results of SEC have already shown that thermolysis gives rise to a considerable amount of low-mass oligomeric species via chain scission processes. Assuming that cyclization reactions occur only to a very small degree during thermolysis, if at all, then the increased concentration of low-mass linear oligomers (due to chain scission) as compared with cyclic oligomers is to be expected.

Increasing pyrolysis times produce increasingly more complex ESI spectra and the polymer distribution as observed by ESI gradually tends towards lower molecular weight. This is presumably not only a consequence of the occurrence of chain scission processes during thermolysis, but also the higher solubility of the lower mass species in the THF/MeOH solvent system.

Clearly, the assignment of degraded polynimmo species from these ESI spectra (Fig. 10) is impossible due to the complexity of the mixture of ions present. Column chromatography was therefore employed to separate the complex mixture of degradation products, as described below.

3.2. Part 2. Spectral characterization of pyrolysed polynimmo following exhaustive column chromatography

The results given above clearly demonstrate that pyrolysed polynimmo comprises a complex mixture of degradation products. Column chromatography was therefore employed to separate this mixture, with the aim of obtaining either pure or at least enriched samples of individual thermal degradation products observed by i.r., at 1729 cm^{-1} (carbonyl product) and 1550 cm^{-1}, thus aiding the characterization of the latter species, tentatively assigned to a nitro-species, by ESI and n.m.r.

Polynimmo (10.0 g) was placed in a glass vial (25.0 cm^3) and pyrolysed in the oven at 130°C for 25 h. The pyrolysate (5.0 g) was dissolved in toluene to give a saturated solution, and column chromatography was carried out as described in the Experimental section. This eluting solution was collected as 15 cm^3 fractions and approximately 250 fractions were collected over a 12 h period.

3.2.1. Infrared spectroscopic characterization of the fractions obtained from column chromatography of pyrolysed PNMMO

Above we show that new absorptions are observed at 1550 and 1729 cm^{-1} in the solution i.r. spectra of polynimmo following pyrolysis. Other new absorptions, thought to be associated with the species absorbing at 1729 cm^{-1}, are also visible in the i.r. difference spectra.

The first 20 fractions obtained from the column chromatography of pyrolysed polynimmo contained solely solvent. The i.r. spectra of the subsequent nine fractions showed absorptions characteristic of undegraded cyclic oligomer. This was substantiated by the ESI spectra of these fractions which show only a single peak due to the cyclic tetramer ion. The i.r. spectra of fractions 30–41 show a new peak of gradually increasing intensity at 1550 cm^{-1}. This peak, tentatively assigned to a nitro-species, gradually decreases in intensity in fractions 42–52. Fig. 11(A) shows the solution ($CDCl_3$) i.r. spectrum of fraction 41.

Only one new peak is visible in this spectrum at

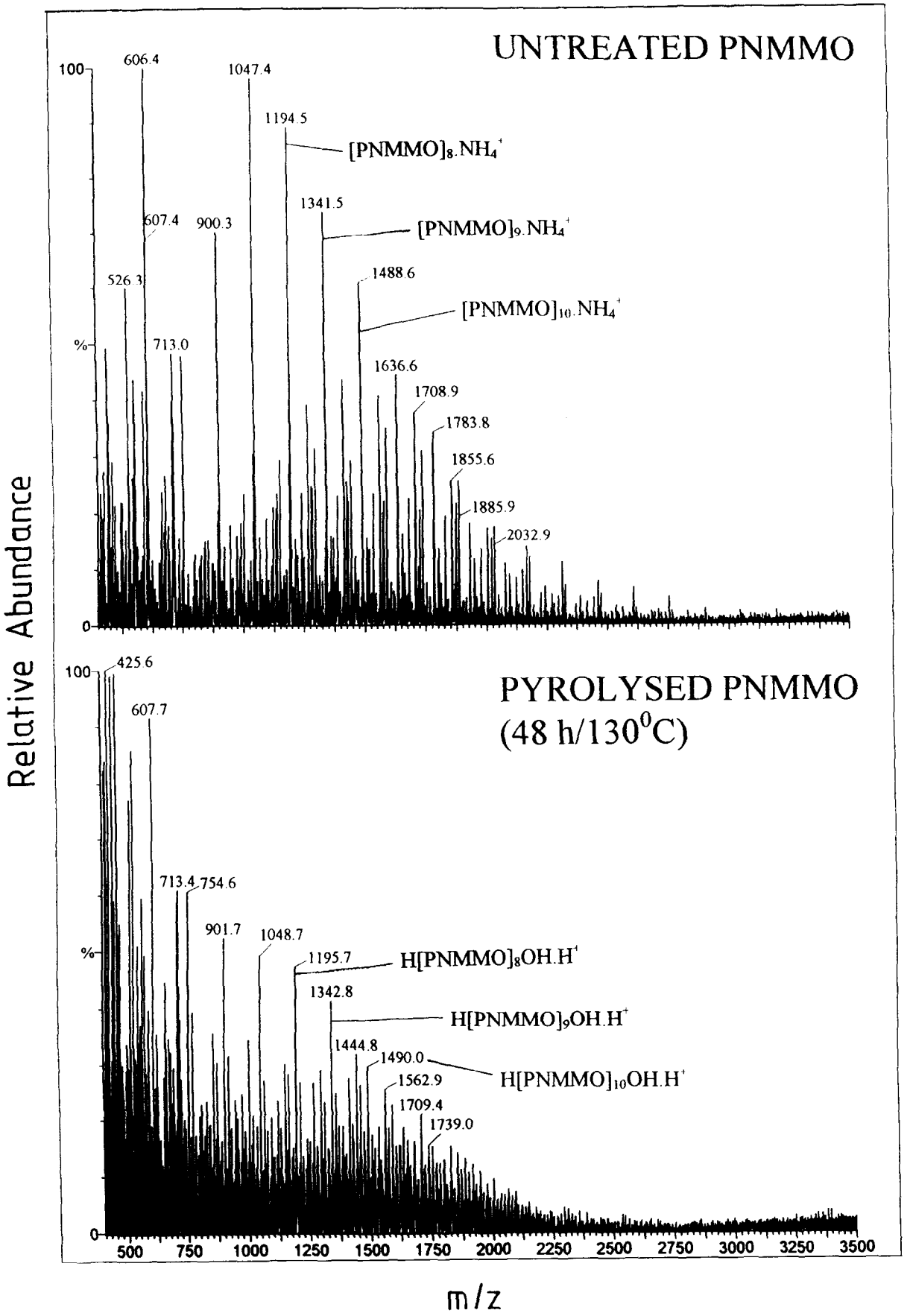

Fig. 10. ESI spectra of (upper) untreated polynimmo and (lower) polynimmo pyrolysed at 130°C for 48 h.

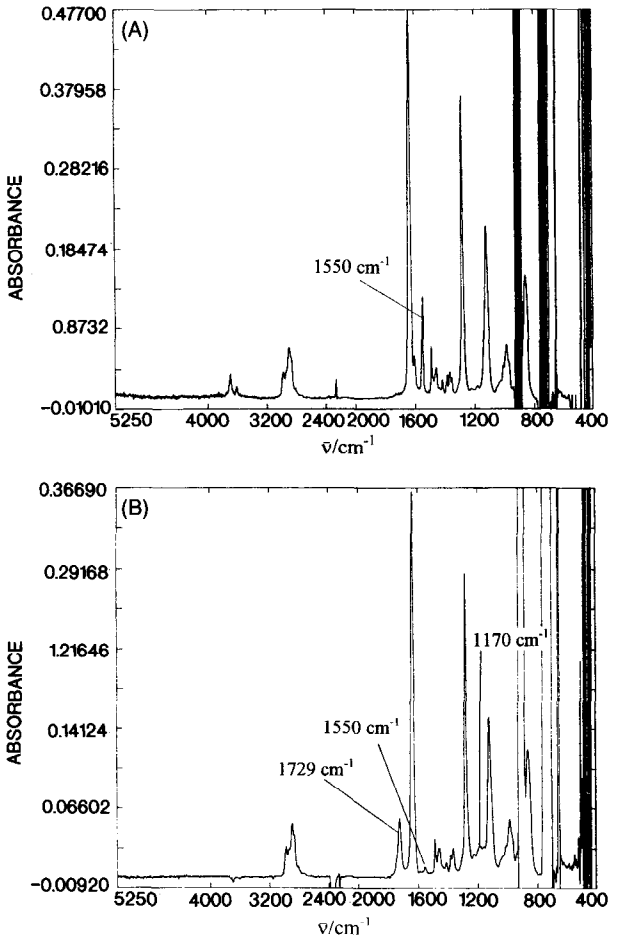

Fig. 11. Solution i.r. spectra ($CDCl_3$) of fractions from column chromatography of pyrolysed polynimmo. (A) Fraction 41; (B) fraction 100.

1550 cm^{-1}, and thus it appears that this sample contains solely the nitro-species and possibly some undegraded oligomer. Clearly, the isolation of this nitro-species confirms, as expected, that it can exist independently of the carbonyl species absorbing at 1729 cm^{-1}.

The i.r. spectra of fractions 53–150 show absorptions for both the 1550 and 1729 cm^{-1} species. The relative intensities of these peaks vary in each spectrum in a non-uniform manner. Fig. 11(B) shows the i.r. spectrum of fraction 100. The ratio of the intensities of the 1729 to 1550 cm^{-1} absorptions is the greatest in this spectrum; the peak at 1729 cm^{-1} is six times as intense as that at 1550 cm^{-1}. A comparison of the i.r. spectra of fractions 40(Fig. 11(A)) and 100 (Fig. 11(B)) shows that the peak due to the carbonyl species at

Table 1
M_n and M_w values obtained by SEC for fractions from column chromatography of pyrolysed polynimmo

Fraction	M_n	M_w
154	1000	3400
169	3000	13 000
193	8300	28 000

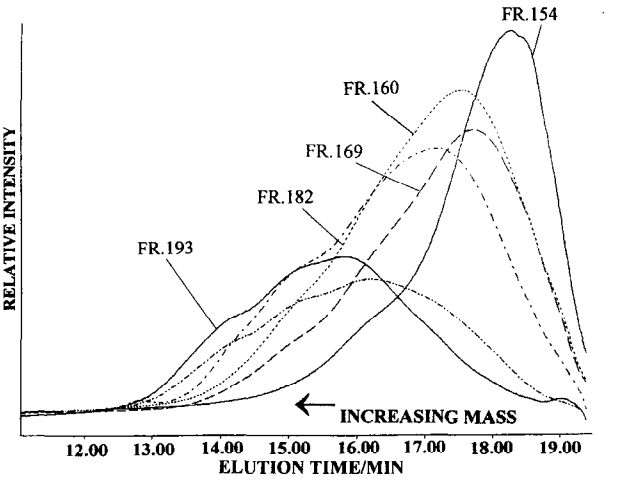

Fig. 12. SEC chromatograms of (late) representative fractions from the column chromatography of pyrolysed polynimmo (25 h/130°C).

1729 cm^{-1} is associated with the absorption around 1170 cm^{-1} which is visible in Fig. 11(B) but not (A). This confirms the assignment of the carbonyl group to a formate ester (see above). The i.r. spectra of fractions 151–220 also show absorptions for both the 1729 and 1550 cm^{-1} species and thus it appears impossible to obtain a sample containing solely the formate ester. Unlike the same absorptions for fractions 53–150, the ratio of the intensities of the 1729 and 1550 cm^{-1} absorptions appears to vary in a uniform manner for fractions 151–220; the intensity of the 1729 cm^{-1} absorption gradually decreases relative to the 1550 cm^{-1} absorption with increasing elution order. Explanation of this variation in the relative concentrations of the species absorbing at 1729 and 1550 cm^{-1} in the i.r. spectra of the eluted fractions is clarified by the SEC and CHN analysis of the fractions, as described and discussed below.

3.2.2. SEC and elemental analytical characterization of fractions obtained from column chromatography of pyrolysed polynimmo

As with the fractions obtained from the column chromatography of untreated polynimmo [4], the higher mass linear oligomers in degraded polynimmo are eluted last. Fig. 12 shows the SEC chromatograms of fractions 154, 160, 169, 182 and 193 obtained from the column chromatography of pyrolysed polynimmo. The chromatograms were run using a high molecular weight column system and equivalent masses of oligomer. In Part 1 we showed that the pyrolysis of polynimmo results in a much wider polymer distribution as observed by SEC. Both Fig. 13 and the molecular weight averages obtained from fractions 154, 169 and 193 (Table 1) clearly illustrate that a good degree of separation of this polymer distribution is possible by column chromatography.

Conversely, the fractions containing the higher mass linear oligomers obtained from the column chromatography of untreated polynimmo show only very small differences in

Table 2
CHN analysis of untreated polynimmo and pyrolysed polynimmo before and after column chromatography

Sample	%C	%H	%N	%O[a]
Untreated (found)	41.02	6.18	9.20	43.60
Untreated (theoretical)	40.82	6.17	9.52	43.50
Pyrolysate (before chromatography)	42.53	6.34	8.53	42.60
Fraction 154	42.10	6.30	8.51	43.09
Fraction 160	42.15	6.30	8.55	43.00
Fraction 169	42.26	6.31	8.63	42.80
Fraction 175	42.42	6.38	8.57	42.63
Fraction 180	42.35	6.34	8.64	42.67
Fraction 187	42.46	6.35	8.61	42.58

[a] Figure obtained by subtraction.

the M_n and M_w values due to the much narrower polymer distribution.

As shown above, the ratio of the intensities of the 1550 and 1729 cm^{-1} absorptions in the i.r. for fractions 150–220 show a trend towards a greater concentration of the species due to the absorption at 1550 cm^{-1} (tentatively assigned to a nitro species) as compared with the species absorbing at 1729 cm^{-1} (formate ester) with increasing elution time. Clearly, SEC analysis of these fractions shows that they contain the linear oligomers of polynimmo, eluted in order of increasing molecular weight. The results of Part 1 have shown that the production of the formate ester species during thermolysis most likely occurs via scission of the C–C bond in the main chain of polynimmo. Thus on average, the fractions containing relatively lower molecular weight oligomer are expected to contain a higher concentration of carbonyl species as compared with the higher molecular weight fractions. The results given below also show that the formation of the species absorbing at 1550 cm^{-1} in the i.r. spectrum does *not* result in chain scission and therefore its concentration would not be expected to vary with the molecular weight of the oligomer. Consequently, the intensity of the absorption at 1550 cm^{-1} relative to the carbonyl absorption (1729 cm^{-1}) is expected to increase with increasing elution time, as we observe. CHN analysis of the fractions further substantiates this (see below).

As shown in Table 2, the percentage of C, H and O in untreated polynimmo shows good agreement with expected values (overall percentage error = 0.5%). The percentage of N is, however, lower than expected (overall percentage error = 3.5%) which may result from the influence of the different end groups present. Calculations were based on the percentage of C, H, N and O in the monomer unit of polynimmo and did not take account of end groups, as the relative amounts of each end group present are impossible to calculate.

As the elution time increases, the percentage of O in the fractions tends to decrease. This can again be explained by the higher concentration of formate ester present in the lower molecular weight species. Many competing reactions make it difficult to see any particular trends in the percentage of C, H and N, although the percentage of N in the pyrolysate before chromatography and in all the fractions is lower than in untreated polymer, presumably due to the loss of NO_x.

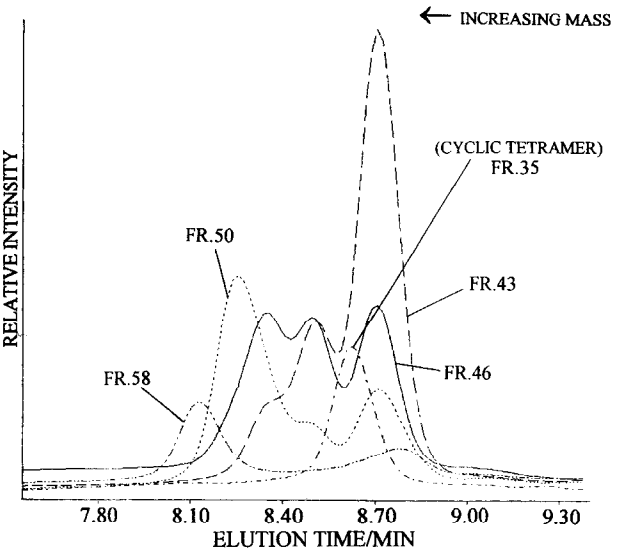

Fig. 13. SEC chromatograms of early fractions, containing predominantly low-mass cyclic oligomers, from the column chromatography of pyrolysed polynimmo (25 h/130°C).

Fig. 13 shows the SEC chromatograms of fractions 35, 43, 46, 50 and 58 obtained from the column chromatography of pyrolysed polynimmo Both the i.r. and ESI spectra of fraction 35 (see above) have shown that this fraction and fractions 21–29 contain solely the cyclic tetramer. This is confirmed by the SEC chromatogram for fraction 35 which shows a single peak with an M_n value identical to that for the cyclic tetramer obtained by column chromatography of untreated polynimmo (see Part 1). Thus, as expected, some cyclic tetramer still remains undegraded.

The mass of oligomer recovered from each of the first 150 fractions obtained from column chromatography was usually approximately 5–10 mg. Consequently, characterization of individual fractions using ESI, SEC, n.m.r. and i.r. was not always feasible, as complete sample recovery was sometimes impossible, particularly for SEC and ESI where the solvents contained added salts and stabilizers. So, although the i.r. spectra show fraction 41 contains the highest concentration of the putative nitro species, the SEC chromatogram of fraction 43 and not 41 is shown in Fig. 13. In any case, the i.r. spectrum of fraction 43 shows a strong absorption at 1550 cm^{-1}. The SEC chromatogram of fraction 43 (Fig. 13) consists of three peaks, decreasing in intensity towards higher mass. The most intense peak in this chromatogram appears at a lower mass than that of the cyclic tetramer (see fraction 35). The column chromatography of untreated polynimmo [4] shows that the cyclic oligomers are eluted in order of increasing molecular

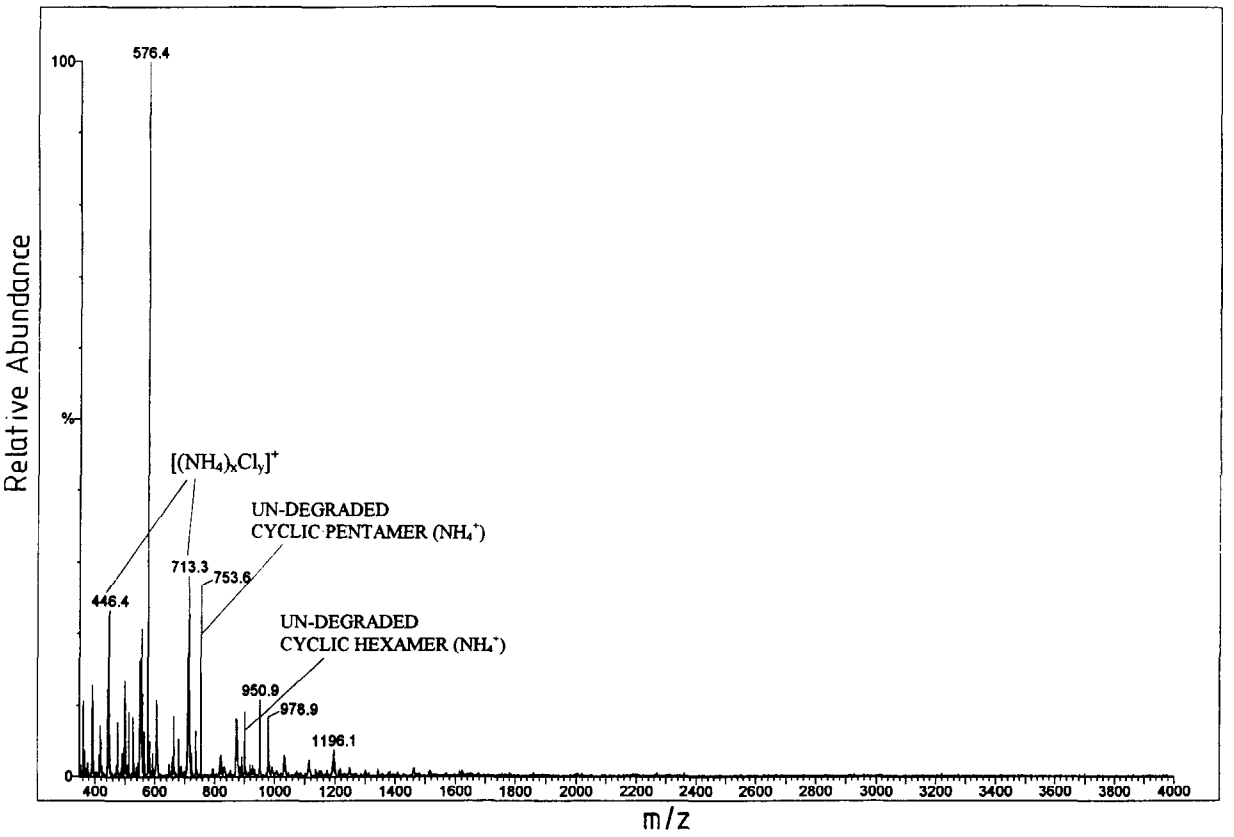

Fig. 14. ESI spectrum of fraction 43, containing predominantly low-mass cyclic oligomers, from the column chromatography of pyrolysed polynimmo.

weight, starting with the cyclic tetramer, prior to the elution of the linear oligomers. Thus, it appears that a new species with a lower molecular weight than that of the cyclic tetramer is present in fraction 43. A comparison of the i.r. spectra and SEC chromatograms for fractions 30–53 shows that this new peak in the chromatograms is present in all the fractions containing the 1550 cm^{-1} peak in the i.r., and the variation in intensity of this new peak in the SEC chromatograms exactly mimics the variation in intensity of the new absorption at 1550 cm^{-1} in the i.r.; the chromatograms of fractions 46 and 50 show that with increasing elution order, the relative intensity of this new peak decreases relative to other peaks as does the absorption at 1550 cm^{-1} in the i.r. This new peak in the chromatograms is thus associated with the species absorbing at 1550 cm^{-1} in the i.r. This species is characterized and assigned using ESI in the next section. Other peaks in the chromatograms can be assigned to undegraded higher mass cyclic homologues by comparing their M_n values to those of the cyclic oligomers obtained by column chromatography of untreated polynimmo.

3.2.3. ESI characterization of the fractions obtained from column chromatography of pyrolysed polynimmo

Fractions 30–52 obtained from the column chromatography of pyrolysed polynimmo contain varying concentrations of the species absorbing at 1550 cm^{-1} in the i.r. The results given below show that this species is associated with a new peak in the SEC chromatograms. Clearly, the identification of this species is vital to the elucidation of the thermal decomposition pathway of polynimmo. The ESI spectra of fractions 30–52 show a new ion peak which varies in intensity in a manner identical to the new peak in the i.r. and SEC chromatograms. Fig. 14 shows the ESI spectrum obtained for fraction 43 using NH_4Cl to promote ionization.

The new ion peak is the most intense peak in this spectrum and is clearly visible at 576.4 Da. Peaks around 446, 552 and 713 Da are attributed to $[(NH_4)_xCl_y]^+$ clusters and the peak at 753.6 Da is assigned to the NH_4^+ adduct of the undegraded cyclic pentamer. The peak due to the cyclic pentamer is also visible in the SEC chromatogram of fraction 43 (Fig. 13). Other peaks in the ESI spectrum of fraction 43 are less than one-tenth as intense as the peak at 576.4 Da and can be assigned to the undegraded linear oligomers of polynimmo by comparison with the ESI spectra of chromatographed untreated polynimmo [4]. The peak at 576.4 Da in the ESI spectrum is later attributed, with the aid of CID, to an NH_4^+ adduct and is thus associated with a species of mass 558.4 Da. The new peak in the SEC chromatograms (Fig. 13) has a mass value just lower than that of the cyclic tetramer (588.4 Da), which strongly suggests that this peak is associated with the new peak at 576.4 Da in the ESI spectrum (Fig. 14). Except for the new peak at 576.4 Da, all the ion peaks in the ESI spectrum can be

assigned to the undegraded cyclic and linear oligomers of polynimmo. Consequently, the species absorbing at 1550 cm^{-1} in the i.r. spectra of fractions 30–52 is most likely to be associated with the ion peak at 576.4 Da in the ESI spectrum. Due to the relatively high concentration of this species in fractions 30–52 as observed by SEC, i.r. and ESI, and its relatively short elution time from the column, it was tenatively assigned to a thermal degradation product of the cyclic tetramer. This was subsequently confirmed by n.m.r. spectrometry (see below). Consequently the ammonium ion adduct peak at 576.4 Da is associated with a compound formed by the loss of 30 Da from the cyclic tetramer. Two candidate molecules of mass 30 Da are NO and CH_2O. However, the abundant loss of formaldehyde from polynimmo during pyrolysis has already been demonstrated using gas-phase i.r. spectroscopy (see above) and CH_2O thus seems the most likely attribution to the species of mass 30 Da. The loss of NO from a nitrate ester would leave a peroxyl radical, the formation of which would involve an unlikely, highly concerted pathway. Loss of formaldehyde from the main chain in the cyclic tetramer must proceed via scission of at least two bonds in the main chain to produce an unstable molecule which will undergo further reaction. The resulting molecule is expected to have a different mass from that observed for the degradation product of the cyclic tetramer and thus an alternative degradation route is likely.

The resulting nitroalkane exhibits an overall loss of 30 Da from the original cyclic tetramer and produces an ion peak due to the ammonium adduct at 576.4 Da as we observe. The strong absorption visible at 1550 cm^{-1} in the i.r. spectra of fractions 30–52 is consistent with the asymmetric stretch of a nitroalkane [17,18]. However the absence of a similarly intense absorption due to the symmetric stretch of the nitroalkane around 1340 cm^{-1} in the i.r. spectrum of fraction 41 (Fig. 11(A)) and i.r. difference spectrum of pyrolysed un-chromatographed polynimmo (Fig. 3) appears at variance with this assignment. Indeed without the ESI results, the absorption at 1550 cm^{-1} could well be attributed to a tertiary nitroso compound which produces only a single absorption around 1600 cm^{-1} in the i.r. However the frequency of the asymmetric and symmetric stretching absorptions of the NO_2 group are highly sensitive to the nature of the attached alkyl group [17,18]; i.r. studies of nitroalkanes reveal that the absorption band due to the symmetric stretch is particularly sensitive and is less strongly-defined as regards frequency and intensity as compared to the antisymmetric stretch [22]. For this same reason there is no clear overall relationship between the frequencies of these two bands in tertiary alkyl nitro compounds [22]. In general, the symmetric absorption is appreciably less intense than the asymmetric absorption as we observe for the nitro species in our studies. A further complication also arises due to the presence of the methyl group on the α-carbon atom of the nitro species, which causes the symmetric absorption to split such that the total intensity is equally divided between the two bands [46]. These two bands generally appear around 1370 and 1395 cm^{-1} and we do find weak absorptions at 1377 and 1394 cm^{-1} in the i.r. difference spectrum of pyrolysed unchromatographed polynimmo (Fig. 3). It was not possible to run i.r. difference spectra of the fractions obtained from column chromatography as it was impossible to calculate the exact relative amounts of oligomer present and thus prepare a background sample. However, as the frequency of the absorption at 1550 cm^{-1} is exactly the same for both the degraded cyclic tetramer and degraded bulk polynimmo samples, the nitro species formed by pyrolysis of the cyclic tetramer is thought to be structurally identical to that formed during pyrolysis of bulk polynimmo.

ESI spectra were also obtained for fraction 100 which appeared to contain a relatively high concentration of the carbonyl species as observed by i.r. spectroscopy (Fig. 11(B)). Fig. 15 shows the ESI spectrum of fraction 100 obtained using NH_4Cl to promote ionization. Six new peaks are visible in this spectrum at 572.6, 589.4, 603.4, 620.4, 870.4 and 1164.4 Da. All other peaks in the spectrum can be assigned to undegraded cyclic and linear oligomers such as the cyclic hexamer, heptamer and octamer at 900.4, 1047.3 and 1194.4 Da, respectively. Although fraction 100 appears to contain a high concentration of the carbonyl species, a low intensity absorption is also visible for the nitro species at 1550 cm^{-1}. No peak is visible for the partly degraded cyclic tetramer at 576.4 Da, but new peaks are visible at 870.4 and 1164.4 Da attributed to nitro formation in the cyclic hexamer and octamer, respectively. Thus, as we expect, nitro formation occurs not only in the cyclic tetramer but also in the higher cyclic homologues.

In addition to the ESI, i.r. and SEC results which all support our assignment of the tertiary nitroalkane in pyrolysed polynimmo, CID experiments were also performed, as detailed below.

3.2.4. CID characterization of the undegraded cyclic tetramer and low-mass thermal degradation products of polynimmo

Fig. 16 shows the CID spectra of both the H^+ adduct of the undegraded cyclic tetramer (589.4 Da) and the NH_4^+ adduct of the nitro species (576.6 Da) produced during thermolysis of polynimmo. The ESI spectra of the nitro species show only a very low abundance of the H^+ as compared to the NH_4^+ adduct and thus it was difficult to obtain reproducible CID spectra of the H^+ adduct. However the CID spectra of the H^+ and NH_4^+ adducts of the undegraded cyclic tetramer are nearly identical and differ only to a small extent in the relative abundances of the product ions. The product ions are considerably more intense in the CID spectrum of the H^+ as compared with NH_4^+ adduct of the cyclic tetramer and thus the CID spectrum of the H^+ adduct of the cyclic tetramer is compared with the NH_4^+ adduct of the nitro species in Fig. 15. The NH_4^+ ion binds more strongly to the cyclic tetramer than does the H^+ ion

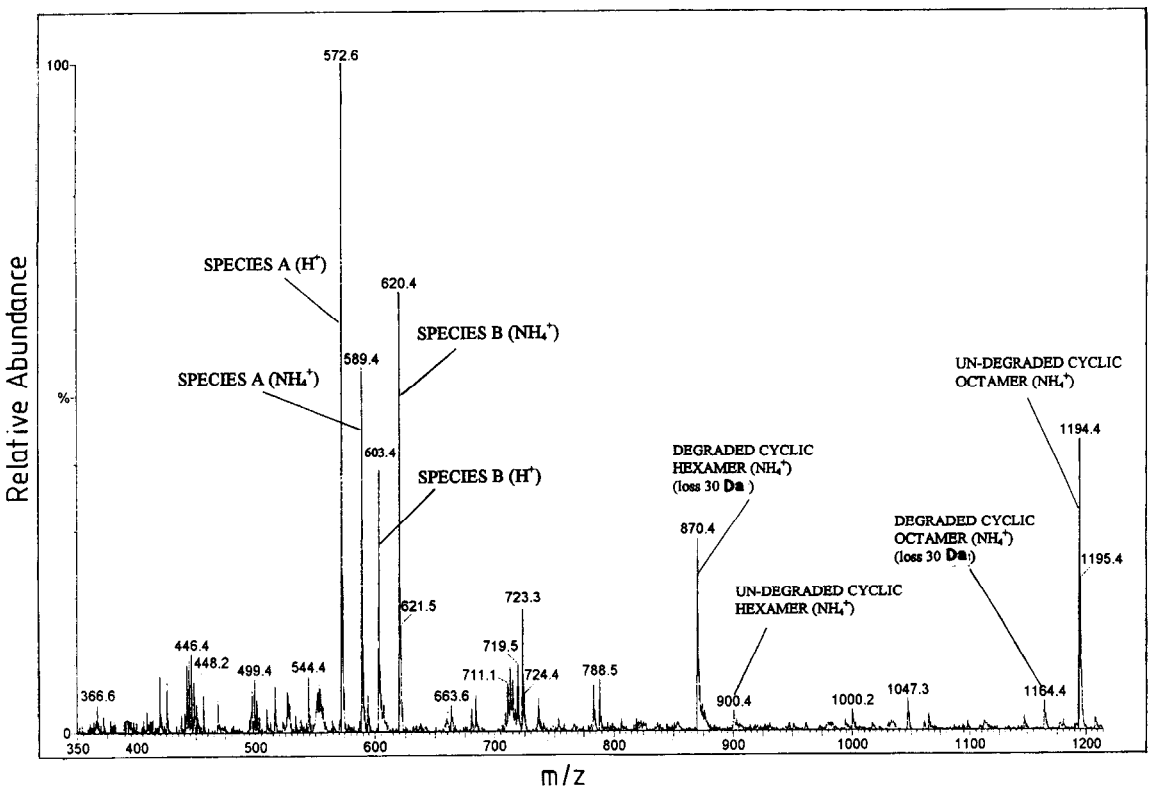

Fig. 15. ESI spectrum of fraction 100, containing relatively large amounts of carbonyl-containing product, from the column chromatography of pyrolysed polynimmo.

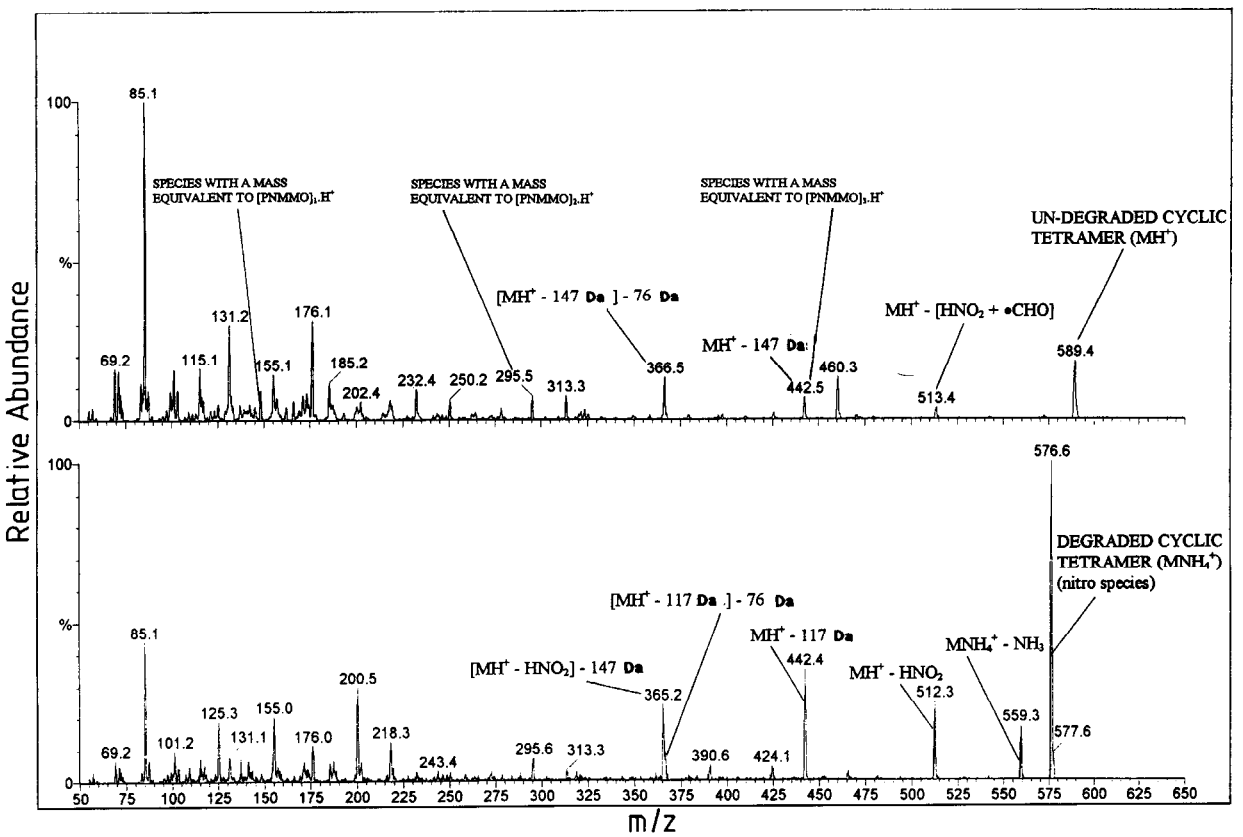

Fig. 16. Collision-induced dissociation ESI mass spectra of the undegraded cyclic tetramer (upper) and the degraded cyclic tetramer (lower).

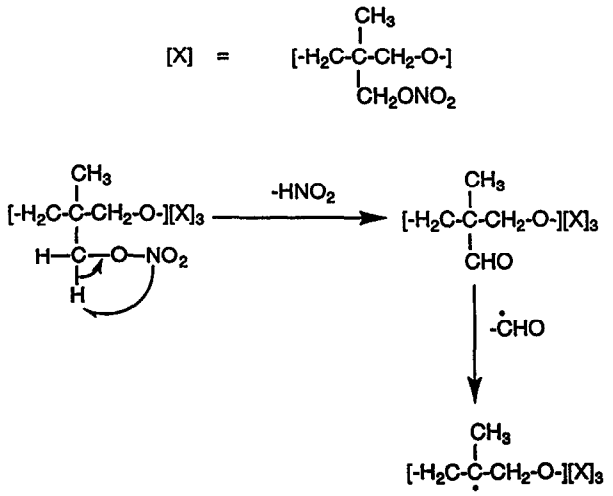

Scheme 2. Fragmentation of a single nitrate ester side-chain in the CID of the cyclic tetramer of polynimmo.

due to the multiple hydrogen bonds that can exist between the ring and side-chain oxygens in the cyclic tetramer and the hydrogen atoms in the NH_4^+ ion. Therefore as expected, the NH_4^+ adduct of the cyclic tetramer is more difficult to fragment via CID as compared with its H^+ counterpart and thus gives a lower abundance of product ions as compared with the parent ion; similar observations are also reported for cyclic and linear polyethers [47,48].

An extensive literature search failed to find any publications relating to the CID of nitrate ester or nitro compounds using ESI. However, various reports concerning the electron impact (EI) mass spectra of aliphatic nitro compounds [49,50], acyclic [51,52] and cyclic [53,54] polyethers and the CID mass spectra of cyclic[55–57] polyether compounds do exist. It is reported that acyclic polyethers, particularly poly(ethylene oxide) and PPO, show product ions resulting from the loss of consecutive monomer units during FAB [51,57], EI [17] and CID [48,55] measurements. The generally accepted mechanism for this loss is 1, 4-hydrogen elimination with concurrent C–O bond cleavage. Cyclic polyethers similarly undergo loss of consecutive monomer units [51] via C–C or C–O bond cleavage, although this process is complicated by the presence of side-groups. The mechanism of loss of monomer units in the cyclic tetramer of polynimmo is thought to differ from that of the simple polyethers which can eliminate neutral species, such as C_2H_4O in the case of poly(ethylene oxide), in a relatively low energy process.

The CID spectra in Fig. 16 show that both the undegraded cyclic tetramer and the nitro species fragment via loss of consecutive monomer units similarly to the cyclic and linear polyethers described above. Species with the same mass as the monomer, dimer and trimer of polynimmo are labelled on the spectra. The main fragmentation pathways are also labelled along with their respective loss in mass. The NH_4^+ adduct of the nitro species (576.6 Da) initially fragments via loss of NH_3 to give the H^+ adduct at 559.3 Da. The loss of

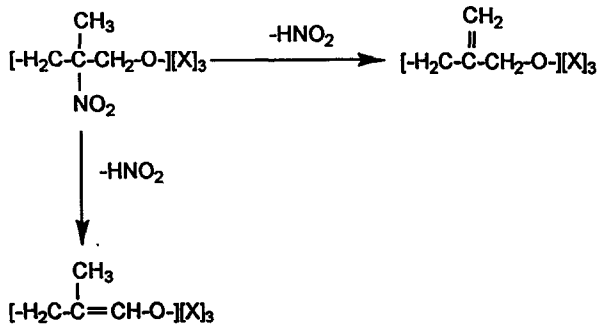

Scheme 3. Fragmentation of the nitro side(chain in the CID of the partially degraded cyclic tetramer.

NH_3 is typical of NH_4^+ adducts [47] and confirms our assignment of the peak at 576.6 Da to an NH_4^+ adduct as opposed to an H^+ adduct. As expected, the H^+ adduct of the undegraded cyclic tetramer (MH^+) does not show a fragment ion at MH^+-17. There is however a prominent peak at MH^+-76 which is consistent with cleavage of the C–C bond adjacent to the ONO_2 group in any one of the four nitrate ester side chains in the cyclic tetramer. Minor peaks at MH^+-47 and MH^+-63 suggest that the consecutive elimination of the two neutral species HNO_2 and $^{\cdot}CHO$ may also play a major (and possibly the major) role in the formation of the species with mass MH^+-76 as shown below in Scheme 2.

Conversely, the H^+ adduct of the nitro species (559.3 Da) shows a fragment ion peak at MH^+-47. In the EI mass spectra of primary and secondary nitroalkanes, the loss of both $^{\cdot}NO_2$ and HNO_2 from the molecular ion (M) is observed but the latter process occurs to a much lesser extent and the M-HNO_2 ion peak is present in only very low abundance as compared to the M-NO_2 ion peak. The EI mass spectra of tertiary nitroalkanes are in most cases different, the main feature being the loss of HNO_2 from the molecular ion giving rise to the highest discernible peaks in the spectra [50]. Clearly, an ion peak at MH^+-47 is observed in the CID mass spectrum of the tentatively assigned nitro species (Fig. 16) thus substantiating our assignment of this thermal degradation product to a tertiary nitro species. The MH^+-46 ion peak is not apparent in this mass spectrum. Aplin et al. [49] show that the loss can occur from either the methylene or the methyl group in 2, 4-dimethyl-2-nitropentane. As with the nitro species, loss of hydrogen may occur via either of the routes shown below in Scheme 3.

Both the undegraded cyclic tetramer and the nitro species show a prominent ion peak for the trimer of NIMMO at 442.4 Da. This ion is thought to originate from the direct fragmentation of the ions at 589.4 and 559.3 Da, respectively, and the mechanism is proposed in Scheme 4.

This mechanism is similarly applicable to the H^+ adduct of the nitro species (559.3 Da), although the presence of the nitro group appears to promote the elimination of the nitro-containing monomer unit. Thus instead of the loss of

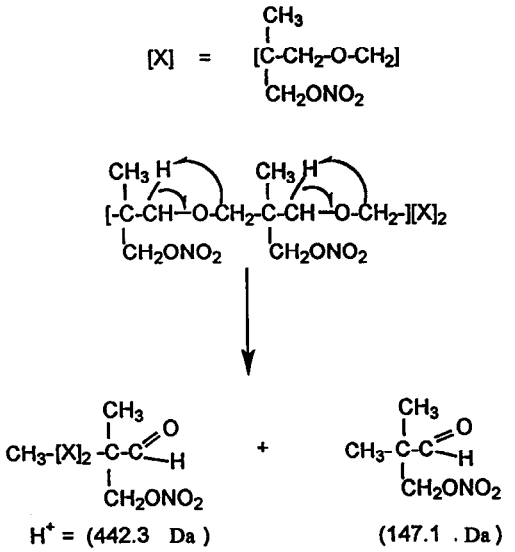

Scheme 4. Proposed mechanism for elimination of a species of mass 147.1 Da, i.e. the same as that of the repeat unit of polynimmo.

147 Da, as observed for the undegraded cyclic tetramer, a loss of 117 Da is observed from the nitro species resulting in a species which exhibits an ion peak at 442.2 Da. Clearly the mass of the nitro side-chain is 30 Da lower than that of the other three nitrate side chains, thus accounting for the loss of 117 Da instead of 147 Da.

The H^+ adduct of a species with a mass equivalent to two polynimmo repeat units is observed at 295.5 Da in the CID spectrum of the undegraded cyclic tetramer and at 295.6 Da in the CID spectrum of the nitro species. We propose that this species is formed by the loss of 147.1 Da from the species with a mass of 442.4 Da in a similar mechanism to that shown in the scheme above. The scheme below shows the mechanism of this loss of 147.1 Da although a species with 147.1 Da would also be lost if the same process were to occur in the adjacent monomer unit. Thus two distinct pathways exist, both of which generate ions with masses of 147.1 and 295.5 Da (Scheme 5).

The prominent ion peak at 366.5 Da in both of the CID spectra shows that the species with a mass of 442.4 not only

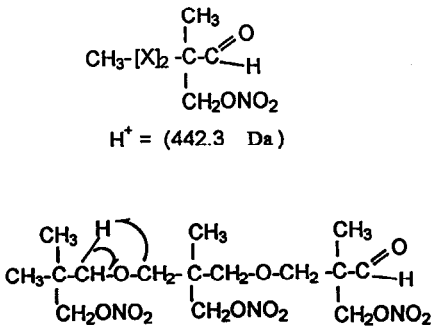

Scheme 5. Mechanism of loss of species with mass 147.1 Da from species of mass 442.4 Da.

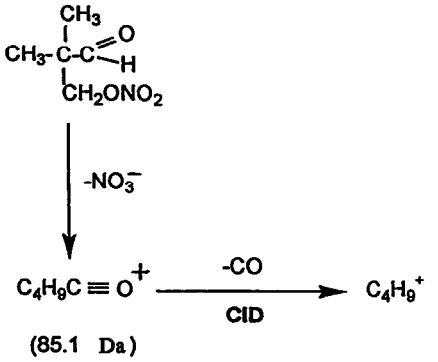

Scheme 6. Formation of acylium ion in the CID of the species of mass 147.1 Da.

eliminates a fragment of mass 147.1, as shown in the mechanism above, but in a parallel process also eliminates a nitrate ester side-chain in a similar process to that in the scheme, i.e. loss of HNO_2 followed by elimination of $CHO^{\cdot}$. The ion peak at 366.5 Da in the CID spectrum of the nitro species is observed only as a shoulder on the peak of mass 365.2 Da, the latter ion being formed by the elimination of 147.1 Da from the species with a mass of 512.3 Da. Clearly the CID spectra of both the cyclic tetramer and the nitro species contain many product ions but most of these result from the consecutive elimination of fragments of mass 147.1 or 76 Da (HNO_2 + $CHO^{\cdot}$).

The fragment of mass 147.1 which is generated in all the proposed schemes above may then eliminate NO_3^- ion and rearrange to give the $C_4H_9CO^+$ ion which shows an intense ion peak at 85.1 Da in both CID spectra (Fig. 16), however there are several alternatives.

The assignment of the species exhibiting an ion peak at 85.1 Da to the $C_4H_9CO^+$ ion (Scheme 6) was substantiated by further CID experiments which showed that this ion fragmented initially by loss of 28 Da, attributed to CO. Lower mass fragments at 43, 41 and 29 Da were assigned to the common fragment ions of hydrocarbons [17] namely $C_3H_7^+$, $C_3H_5^+$ and $C_2H_5^+$, respectively.

The fragmentation schemes shown above account for the main fragmentation pathways of both species but are not completely exhaustive. Clearly the importance of the CID experiment was to establish the presence of a nitro group attached to a tertiary carbon and this was substantiated by the preferential loss of HNO_2 (47 Da) from the H^+adduct at 559.3 Da.

3.2.5. N.m.r. characterization of the fractions obtained from column chromatography of pyrolysed polynimmo

Fig. 17(A) and (B), respectively, shows the ^1H and ^{13}C n.m.r. spectra of fraction 43 which contains a relatively high concentration of the tertiary nitro species as characterized by SEC and ESI. Three distinct new resonances are visible in the ^{13}C n.m.r. spectrum around 20.4, 70.1 and 87.7 ppm. A DEPT experiment reveals resonances as follows: 20.4 ppm, methyl; 70.1 ppm, methylene; and 87.7 ppm,

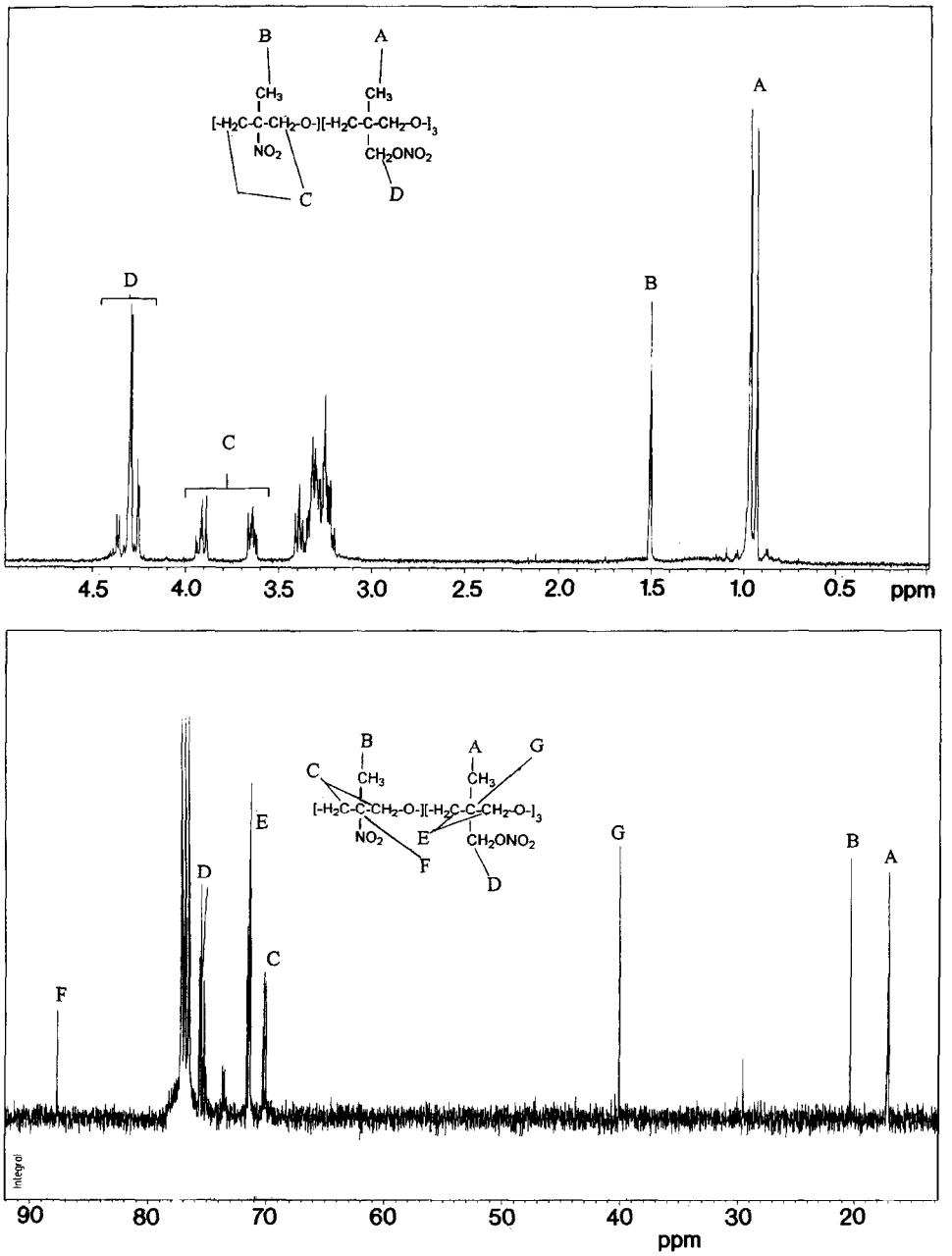

Fig. 17. N.m.r. spectra of fraction 43 from the column chromatography of pyrolysed polynimmo. (A) 400 MHz ^{1}H spectrum; (B) ^{13}C spectrum run on AC 400 spectrometer.

quaternary C. Consequently the resonance at 87.7 ppm is attributed to the quaternary carbon directly attached to the NO_2 group. The chemical shift of this carbon closely matches that for C–NO_2 in 2-methyl-2-nitropropane (85.0 ppm) and the assignment is further substantiated by the ratio of the integrals of the resonances due to the tertiary carbons at 87.7 and 40.1 ppm (the latter refers to the tertiary carbon attached to the unchanged nitrate ester group). This ratio is 0.55:0.15 = 3.7:1 and is, as expected, slightly greater than the 3:1 ratio predicted for the nitro species of the cyclic tetramer due to the presence of much smaller amounts of undegraded cyclic pentamer/hexamer and linear oligomers (as shown by ESI and SEC above). The presence of undegraded cyclic pentamer and hexamer is clearly evidenced in the ^{13}C n.m.r. by the peaks around 73.6 ppm due to the ring methylenes in these two compounds. The new methyl peak at 20.4 ppm is attributed to the methyl group β to the nitro group and, as for the tertiary carbons, the ratio of the integrals of this methyl to the relatively unaltered methyls around 17 ppm is 0.33:1.18 ≡ 1:3.6. Both the ^{1}H and ^{13}C n.m.r. chemical shifts of the new methyl group closely match those for a methyl attached β to a nitro group [17]. The new set of peaks around 70.2 ppm are attributed to the two perturbed methylenes attached β to

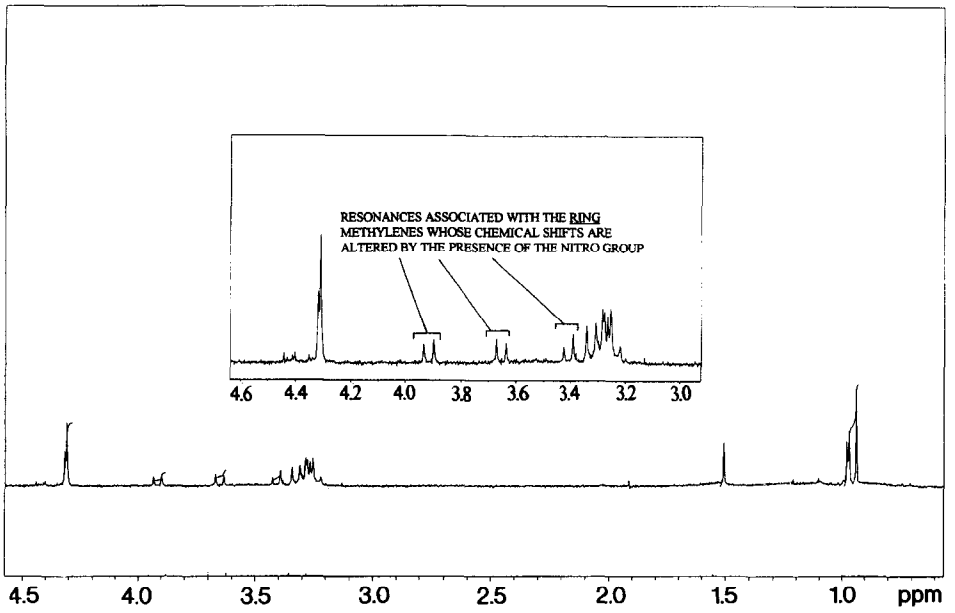

Fig. 18. 250 MHz ^{1}H spectrum of fraction 38 from the column chromatography of pyrolysed polynimmo.

the nitro group and like the new methyl and tertiary carbons, the ratio of their integrals to the six relatively unperturbed methylenes around 71.4 ppm is approximately 1:3.3. Their shift to higher field is attributed to an increased number of γ-gauche effects between the nitro group and the methylene carbons. Thus the *two* oxygens on the nitro group gamma to these methylene carbons may exert a greater γ-gauche effect than the *single* oxygen in the original nitrate ester side chains, resulting in a shift to higher field. The four hydrogens on the two perturbed methylenes β to the nitro group are clearly visible in the ^{1}H n.m.r. (Fig. 17(A)) spectrum of the degraded fraction and exhibit the expected AB system around 3.9 and 3.6 ppm. The coupling constant for this system is more easily extracted from the ^{1}H n.m.r. spectra of fractions containing lower concentrations of the nitro species due to the fewer number of peaks observed for the AB system. There is also a new set of resonances present in the ^{1}H n.m.r. spectrum obtained for a fraction with a lower elution time than that of the fraction 43 above. The coupling constant measured from the resonances around 3.6 and 3.9 ppm is 7.7 Hz and the chemical shift difference is approximately 0.25 ppm. The ^{1}H n.m.r. spectrum (Fig. 18) also shows that the new set of resonances around 3.4 ppm can be attributed to another AB system. Clearly only one set of peaks are visible for this AB system, but the other set are thought to be 'hidden' under the resonances due to the relatively unperturbed methylenes around 3.3 ppm. The coupling constant for this AB system is exactly the same as that measured for the AB system around 3.6 and 3.9 ppm, i.e. 7.7 Hz. The chemical shift difference cannot be measured here but it must be less than that observed for the previous AB system (0.25 ppm) as no resonances with a chemical shift difference of more than 0.20 ppm, except those for the methyl hydrogens, are visible at higher field. The ratio of the integrals of each of the new set of peaks around 3.4, 3.6 and 3.9 ppm in the ^{1}H n.m.r. spectrum (Fig. 17(A)) is ca 1:1:1 and consequently the resonances around 3.4 ppm *and* their associated resonances 'hidden' under the methylene protons around 3.3 ppm are attributed to the hydrogens on the methylene carbons four bonds away from the nitro group. These hydrogens will be influenced to a lesser extent than the hydrogens on the methylenes β to the nitro group and thus both their chemical shift and chemical shift separation will be less but their coupling constant is, as expected, the same. All the resonances due to the methyl and methylene carbons and hydrogens and the tertiary carbons over four bonds away from the nitro group show, as expected, a greater number of resonances than in the undegraded cyclic tetramer due to the relative decrease in the symmetry of the tetramer ring and the reduced influence of the nitro group. Thus, the i.r., SEC, ESI and n.m.r. results for the nitro species of the cyclic tetramer all substantiate the assignment of the thermal degradation product of the cyclic tetramer to a tertiary nitro species.

The assignment of the tertiary nitro group in the cyclic tetramer of polynimmo is extended to linear polynimmo where the same absorption at 1550 cm^{-1} is observed in the solution i.r. spectrum of pyrolysed polynimmo. The peak due to the tertiary carbon α to the nitro group in pyrolysed polynimmo is visible around 89.4 ppm (see Fig. 4(B)) in the ^{13}C n.m.r. spectra instead of at 87.7 ppm as observed for the nitro species of the cyclic tetramer. The shift difference of less than 2 ppm can be attributed to small differences in bond lengths and angles between the linear and cyclic forms of polynimmo. The assignment of this quaternary carbon in linear pyrolysed polynimmo was

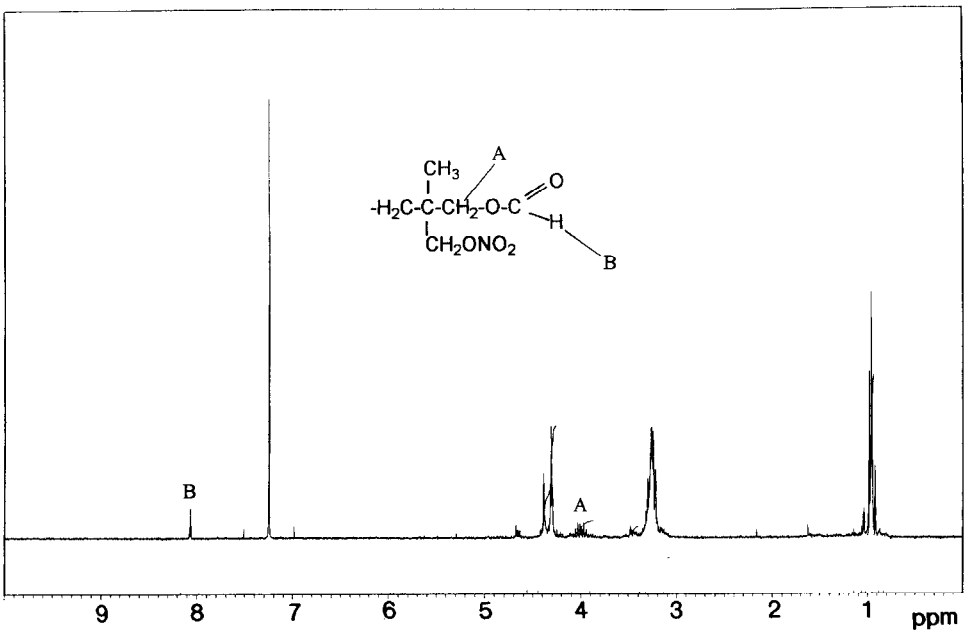

Fig. 19. 400 MHz ^{1}spectrum of fraction 100, containing relatively large amounts of carbonyl-containing product, from the chromatography column of pyrolysed polynimmo.

confirmed by a two-dimensional $^{1}H-^{13}C$ correlation experiment which showed that the resonance at 89.4 ppm in the ^{13}C n.m.r. spectrum of pyrolysed un-chromatographed polynimmo (Fig. 4(B) and Fig. 6) disappears in the two-dimensional experiment (Fig. 5) as no hydrogens are associated with this carbon atom. The relatively strong intensity of the resonance due to this tertiary carbon can be attributed to relaxation effects which also lead to a resonance of relatively strong intensity for the tertiary carbon in untreated polynimmo (Fig. 4(B)). The resonance due to the methyl group β to the nitro group in linear polynimmo is clearly visible in the ^{13}C n.m.r. spectrum of pyrolysed polynimmo at 18.5 ppm (see Fig. 4(B) and Fig. 6) and similarly to the cyclic nitro species, a two-dimensional $^{1}H-^{13}C$ n.m.r. correlation experiment shows that this resonance is associated with the new resonance around 1.5 ppm in the ^{1}H n.m.r. spectrum of pyrolysed polynimmo. The resonance around 18.5 ppm in the ^{13}C n.m.r. spectrum increases in intensity at approximately the same rate as the tertiary carbon at 89.4 ppm. The methylene carbons β to the nitro group in pyrolysed linear polynimmo are tentatively assigned to the new resonances around 65–74 ppm in the ^{13}C n.m.r. spectrum of pyrolysed polynimmo (see Fig. 4(B) and Fig. 6). The shift to higher field is attributed, as for the cyclic nitro species, to increased γ-gauche effects caused by the two oxygens in the nitro group γ to the methylene carbons. Two-dimensional n.m.r. experiments show that all the resonances around 65–74 ppm are attributable to methylene and tertiary carbons and consequently it is difficult to assign individual resonances, although as discussed earlier alcohol species show resonances in this region. The formation of the formate ester species during pyrolysis of polynimmo will also result in a different chemical shift for the methylene carbons γ to the carbonyl oxygen:

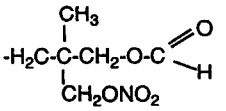

As only a relatively small amount (as determined by integration) of methylenes are shifted to lower field in the ^{13}C n.m.r. spectrum of pyrolysed polynimmo, the new resonances around 65–74 ppm are also attributed to the methylene carbons γ to the carbonyl oxygen which are shifted to higher field due to the γ-gauche effect of the carbonyl oxygen.

As we have shown, the solution i.r. spectrum of fraction 100 (Fig. 11(B)) shows that this fraction contains a relatively high concentration of the formate ester species (1729 cm^{-1}, 1170 cm^{-1}). The ESI spectrum of this fraction (Fig. 15) shows four new peaks at 572.6, 589.4, 603.4 and 620.4 Da. It was only possible to obtain approximately 4 mg of this carbonyl enriched fraction via column chromatography of pyrolysed polynimmo and consequently analysis via SEC or ^{13}C n.m.r. spectroscopy was impossible. However (Fig. 19) shows the 400 MHz ^{1}H n.m.r. spectrum of this fraction. The resonance due to the formate hydrogen is clearly visible around 8.05 ppm as are the resonances due to the hydrogens on the methylene carbon β to the carbonyl group around 4.0 ppm. As expected, the ratio of the integrals of the methylene to the formate hydrogens is 2:1 and the methylene hydrogens show a complex splitting pattern due to their proximity to the carbonyl group and the asymmetric carbon. The resonances due to the methyl, the main

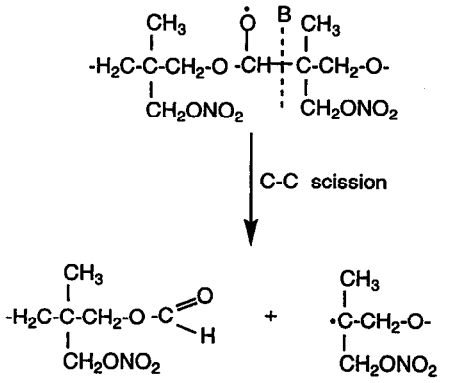

Scheme 7. Scission process in the pyrolysis of polynimmo.

chain and the side-chain methylene hydrogens are clearly visible around 1.0, 3.2 and 4.3 ppm, respectively. CID experiments show that the four new peaks at 572.6, 589.4, 603.4 and 620.4 Da in the ESI spectrum of fraction 100 (Fig. 15) are associated with the H^+ and NH_4^+ adducts of two different species, namely species A and species B. However, without the aid of ^{13}C n.m.r. spectroscopy it is impossible to positively assign either of these two species to cyclic or linear compounds. The CID spectra of the H^+ and NH_4^+ adducts at 603.4 and 620.4 Da in the ESI spectrum of fraction 100 show some similar fragmentation pathways to those observed for the undegraded cyclic tetramer such as the loss of HNO_2 and HCO. However many dissimilar pathways also exist giving rise to a complex CID spectrum containing numerous ion peaks and making identification of individual species very difficult. However the CID spectra of the H^+ and NH_4^+ adducts at 572.6 and 589.4 Da in the ESI spectrum of fraction 100 contain fewer peaks than the CID spectra of the previous adducts (603.4 and 620.4 Da) and importantly show a fragment ion at MH^+-28. Common fragment ions of mass 28 Da are C_2H_4 and CO. As both the solution i.r. and ^1H n.m.r. spectra of fraction 100 point towards the presence of a relatively high concentration of formate ester in this fraction, the fragment ion is attributed to the loss of carbon monoxide from the formate ester and indeed acyclic formate esters are reported [57–59] to fragment via loss of CO. Although the species associated with the H^+ (572.6 Da) and NH_4^+ (589.6 Da) adducts of the formate ester species eluted from the column in our work cannot be positively assigned to an acyclic species, it is unlikely that a formate ester group can be generated in any one of the cyclic homologues of polynimmo without the occurrence of chain scission. Thus although complete analysis of the n.m.r. and ESI spectra is not possible, the i.r., n.m.r. and ESI (CID) results all suggest that the column chromatography of pyrolysed polynimmo has resulted in the separation and characterization of a relatively pure sample of one of the major oxidation products of polynimmo, the formate ester.

Analysis of the fractions eluted from the column chromatography of pyrolysed polynimmo using SEC, i.r., n.m.r. and ESI (CID) has shown that it consists of a complex mixture of undegraded and degraded oligomers. Clearly however the presence of low-mass cyclic and linear oligomers (soluble in the THF/MeOH solvent system) in both the degraded and undegraded polymer allows the characterization of the thermal degradation products of polynimmo via ESI and CID.

We performed several column chromatographic separations of pyrolysed polynimmo and repeat results verified our original assignments of the degradation products in pyrolysed polynimmo.

4. Conclusions

Polynimmo was pyrolysed at temperatures in excess of 90°C and subject to a wide variety of physical techniques. It darkens in colour and becomes gradually more viscous with increasing pyrolysis times, and SEC chromatograms show that both chain scission and cross-linking reactions are taking place. Thermal degradation results in the gradual increase in intensity of two main new absorptions around 1729 and 1550 cm^{-1} in the solution i.r. spectrum of polynimmo. The band at 1729 cm^{-1} is attributed to the carbonyl group in a formate ester and the formate proton and carbonyl carbon associated with this compound are clearly visible in the ^1H and ^{13}C n.m.r. spectrum at 8.1 and 162 ppm, respectively, and can be cross-correlated by two-dimensional n.m.r. The formation of a formate ester species is consistent with the oxidation of the main chain methylenes to form a secondary alkoxy radical which undergoes C–C bond scission adjacent to the alkoxy radical (Scheme 7).

This oxidation mechanism is found to bear many similarities with those of other polyethers such as poly(ethylene oxide) and PPO which similarly form secondary alkoxy radicals and undergo C–C bond scission. Tertiary alcohols formed during the pyrolysis of polynimmo are proposed to originate from the oxidation of the tertiary carbon-centred radical shown above.

400 MHz ^1H and ^{13}C n.m.r. spectra of pyrolysed polynimmo show very low intensity resonances around 9.5 and 205 ppm, respectively, indicating that relatively small amounts of aldehyde species are also produced during pyrolysis. Aldehyde species may result from the oxidation of the main chain or side chain methylenes and it is not clear which of these mechanistic routes leads to aldehyde formation. If the oxidation site is the main chain methylenes then the secondary alkoxy radical shown in the scheme above does undergo some C–O bond scission adjacent to the alkoxy radical to generate an aldehyde but to a much lesser extent than C–C bond scission. Alternatively if the oxidation site is the side chain methylenes then alkoxy radical formation results in the elimination of ONO_2 to generate an aldehyde.

The new absorption at 1550 cm^{-1} in the i.r. spectrum of pyrolysed polynimmo is attributed to the asymmetric stretch

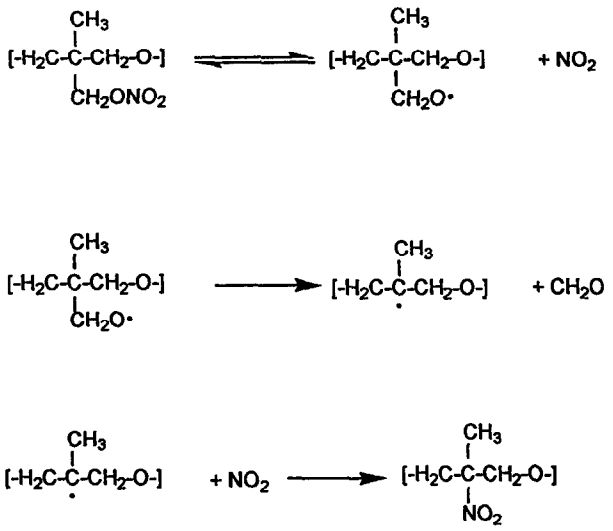

Scheme 8. Mechanism of formation of a nitro-compound from the pyrolysis of polynimmo

of a nitro group attached to a tertiary carbon. The symmetric stretch, which can only be observed in i.r. difference spectra, is weak due to various factors such as the splitting of this absorption by the methyl group β to the nitro moiety. We propose that this nitro species is formed by the recombination of NO_2 following the loss of NO_2 and subsequent elimination of CH_2O from the polynimmo side-chains (Scheme 8).

Numerous chromatographic separations of pyrolysed polynimmo eventually yielded a single fraction of the nitro species of sufficient purity and quantity for analysis. The assignment of this tertiary nitroalkane was then confirmed by ESI mass spectrometry and spectroscopic characterization of this fraction. ^{13}C n.m.r. measurements confirmed that this nitro species was attributable to a compound formed by the decomposition of the cyclic tetramer where one of the four nitrate ester side chains had decomposed, as shown in the scheme above, to generate a nitro group attached to a tertiary carbon. CID experiments showed that the nitro species eliminated HNO_2 which is consistent with a tertiary nitroalkane.

Our degradation mechanism for the formation of the tertiary nitroalkane in polynimmo bears many similarities with the findings of Hiskey et al. [12] who propose that neopentanol nitrate thermally degrades via a similar mechanism to yield the tertiary nitroalkane, 2-methyl-2-nitropropane.

Our degradation mechanism for the formation of the nitroalkane in polynimmo was substantiated by the presence of significant amounts of $CH_2O(g)$ in the pyrolysis gases of polynimmo and the detection of a gradually increasing concentration of a nitroxide radical during pyrolysis of polynimmo. We propose that the nitroxide radical is generated by the reaction of the newly formed tertiary nitroalkane with alkyl polymer radicals.

Although the gradual increase in intensity of an absorption around 1550 cm^{-1} was generally observed in the i.r. spectrum of pyrolysed polynimmo during pyrolysis, the position of this new band was found to vary depending on the experimental conditions. Thus an absorption was observed around 1572 cm^{-1} during the pyrolysis of thin films of polynimmo and this band eventually merged with the band around 1550 cm^{-1} to give a net absorption at 1550 cm^{-1}. Photolysis produced an absorption around 1562 cm^{-1} and the position of this band was also found to vary according to the photolysis conditions. Thus it appears that more than one nitro species is produced and indeed, absorptions around 1550 cm^{-1} in the i.r. spectrum could also be associated with nitroso species. Nitrogen monoxide (NO) could be formed by the reduction of $NO_2(g)$ by $CH_2O(g)$, both of which are formed in significant quantities during the pyrolysis of polynimmo, or NO may result from the decomposition of the tertiary nitroalkane. Nitroso species can then be produced by the recombination of NO with carbon-centred radicals in polynimmo. However, both primary and secondary nitroso species are generally very unstable and undergo dimerization. Tertiary nitroso species are somewhat more stable than primary or secondary nitroso species but they are generally either blue in colour, or if they are sterically hindered, they undergo dimerization [60]. Thus it appears that the formation of nitroso species during the pyrolysis of polynimmo is less likely than the formation of nitro species. Consequently, nitro species in slightly different environments may account for the appearance of more than one absorption due to the asymmetric stretch of the nitro group around 1550–1575 cm^{-1} in the i.r. spectrum and often more than one resonance around 90 ppm in the ^{13}C n.m.r. spectrum due to the carbon atom directly attached to the nitro group.

Acknowledgements

We thank the Defence Research Agency for a studentship to Z.B. Dr. D.M. Haddleton is thanked for access to the SEC equipment and Dr. O.W. Howarth's help with analysing the n.m.r. spectra is gratefully acknowledged. Special thanks are due to Professor K.R. Jennings and Dr. A. Buzy for assistance with the ESI measurements.

References

[1] Bunyan P, Cunliffe AV, Davis A. Proceedings of the 16th International Seminar on Pyrotechnics, 24–28 June 1991, Jänköping, Sweden, p.7.

[2] Bunyan P, Cunliffe AV, Davies A, Kirby FA. Polym Degrad Stab 1993;40:239.

[3] Wirpsza Z. Polyurethanes: chemistry, technology and applications. Chichester: Ellis Horwood, 1993.

[4] Barton Z, Kemp TJ, Buzy A, Jennings KR, Cunliffe AV. Polymer 1997;38:1957.

[5] Staehli R, Broennimann E, Stalder C, Sopranetti A. 20th International

Annual Conference, ICT 1989, Environ Test 90s, 1989, pp. 20/1–20/16.
[6] Shawki SM, El-Hadad MA, Said AM. 21st International Annual Conference, ICT 1990, Technol Polym Comp Energ Mater, 1990:76/1–76/9.
[7] Farber M, Harris SP, Srivastava RD. Department of Navy Office of Naval Research, Arlington, VA, Report AD-A168611, 1986.
[8] Chen JK, Brill TB. Combust Flame 1991;85:479.
[9] Oyumi Y, Brill TB. Combust Flame 1986;66:9.
[10] Chen JK, Brill TB. Thermochim Acta 1991;181:71.
[11] Quinchon J, Tranchant J. Nitrocelluloses. Chichester: Ellis Horwood, 1989.
[12] Hiskey MA, Brower KR, Oxley JC. J Phys Chem 1991;95:3955.
[13] Ambroz HB, Kemp TJ. J Chem Soc Perkin II 1979:1420.
[14] Schoolenberg GE, Vink P Polymer 1991;32:432.
[15] Delprat P, Gardette J-L Polymer 1993;34:933.
[16] Barr-Kumarakulasinghe SA. Polymer 1994;35:995.
[17] Silverstein RM, Bassler GC, Morrill TC. Spectrometric identification of organic compounds, 5th edn. New York: Wiley, 1991:127.
[18] Pouchert CJ, editor. Aldrich Library of infrared spectra. Aldrich Chemical Co., 1970.
[19] Williams DH, Fleming I. Spectroscopic methods in organic chemistry, 5th edn. London: McGraw-Hill, 1995.
[20] Griffiths PJ, Hughes JH, Park GS. Eur Polym J 1993;29:437.
[21] Thompson HW, Torkington P. J Chem Soc 1945:640.
[22] Bellamy LJ. Infrared spectra of complex molecules, vol. I, chap. 17, 3rd edn. London: Chapman and Hall, 1975.
[23] Ham S, Kim C, Kwon D. Polym Degrad Stab 1995;47:203.
[24] Bielski BHJ, Gebicki JM. Atlas of ESR spectra. New York: Academic Press, 1967.
[25] Alger RS. Electron paramagnetic resonance. New York: Interscience, 1968.
[26] Myers GH, Easley WC, Zilles BA. J Chem Phys 1970;53:1181.
[27] Poole CP. Electron spin resonance, 2nd edn. New York: Wiley–Interscience, 1983.
[28] Adrian FJ. J Chem Phys 1962;36:1692.
[29] Symons MCR. Chemical and biochemical aspects of electron spin resonance spectroscopy. New York: Van Nostrand, 1978, Chaps 5 and 7.
[30] Chen W-P, Kenney DJ, Frisch KC, Wong S-W, Moore R. Polym J Sci: Part B: Polym. Phys. 1991;29:1513.
[31] Berliner LJ. Spin labeling. New York: Academic Press, 1976, Chaps 3 and 6.
[32] Yamauchi J, Ando H, Yamaoko A. Macromol. Chem Rapid Commun 1993;14:13.
[33] Ranby B, Rabek JF. ESR spectrometry in polymer research. Berlin: Springer, 1977, Chap. 7.
[34] Kinoshita R, Teramoto Y, Yoshida H. Thermochim Acta 1993;222:45.
[35] Chen JK, Brill TB. Combust Flame 1991;87:157.
[36] Pierson RH, Fletcher AN, Gantz EC. J Anal Chem 1956;28:1218.
[37] Nightingale RE, Downie AR, Rotenberg DL, Crawford B, Ogg RA. J Phys Chem 1954;58:1047.
[38] Brechignac C, Johns JWC, McKeller ARW, Wong M. J Mol Spectrom 1982;96:353.
[39] Fateley WG, Bent HA, Crawford B. J Chem Phys 1959;31:204.
[40] Weston RE. J Chem Phys 1957;26:1248.
[41] Chen JK, Brill TB. Combust Flame 1993;94:70.
[42] Oyumi Y, Brill TB. Combust Flame 1987;68:209.
[43] Oyumi Y, Brill TB. Combust Flame 1985;62:213.
[44] Gray P, Rathbone P, Williams A. J Chem Soc 1960:3932.
[45] Brill TB, James KJ. Chem Rev 1993;93:2667.
[46] Eckstein Z, Gluzinski P, Sobotka W, Urbanski T. J Chem Soc 1961:1370.
[47] Liou C-C, Wu H-F, Brodbelt J. Am Soc Mass Spectrom 1994;5:260.
[48] Selby TL, Wesdemiotis C, Lattimer RP. J Am Soc Mass Spectrom 1994;5:1081.
[49] Aplin RT, Fischer M, Becher D, Budzikiewicz H, Djerassi C. J Am Chem Soc 1965;87:4888.
[50] Konopski L, Grela K. J Org Mass Spectrom 1992;27:741.
[51] Jaeger DA, Whitney RR. J Org Chem 1975;40:92.
[52] Bose AK, Prakash O, Yuan Hu G, Edasery J. J Org Chem 1983;48:1782.
[53] Lattimer RP. J. Am. Soc. Mass Spectrom 1992;3:225.
[54] Lattimer RP, Munster H, Budzikiewicz H. Int J Mass Spectrom Ion Processes 1989;90:119.
[55] Maleknia S, Liou C-C, Brodbelt J. J Org Mass Spectrom 1991;26:997.
[56] Curcuruto O, Traldi P, Moneti G, Corda L, Podda G. J Org Mass Spectrom 1991;26:713.
[57] Budzikiewicz H, Djerassi C, Williams D. Mass spectrometry of organic compounds. CA: Holden-Day, 1967.
[58] Kawashiro K, Morimoto S, Yoshida H. Bull Chem Soc Jpn 1984;57:1097.
[59] Heinrich N, Drewello T, Burgers P, Morrow J. J Am Chem Soc 1992;114:3776.
[60] Sidgwick NV. In: Taylor TWJ, Baker W, editors. The organic chemistry of nitrogen, 2nd ed. Oxford: Oxford University Press, 1949.